CANADA
DEPARTMENT OF MINES AND TECHNICAL SURVEYS
Dominion Observatories

PUBLICATIONS

of the

DOMINION OBSERVATORY

OTTAWA

Volume XXVI · No. 7

A STUDY OF THE GEOPHYSICAL AND GEODETIC IMPLICATIONS OF GRAVITY DATA FOR CANADA

Yasuo Shimazu

Price $1.25

ROGER DUHAMEL, F.R.S.C.
QUEEN'S PRINTER AND CONTROLLER OF STATIONERY
OTTAWA, 1962

A Study of the Geophysical and Geodetic Implications of Gravity Data for Canada

YASUO SHIMAZU

ABSTRACT—Making use of Bouguer anomalies and corresponding surface elevations in Canada, investigations have been made of the physical state of the earth's crust, the distribution of isostatic anomalies, undulations of the crust-mantle boundary, deflections from the vertical and undulations of geoidal heights. A modification of Tsuboi's method —which assumes that a variation in the gravity is caused by the anomalous mass distributions at the base of the crust —is used in this study and computational methods are outlined in Section I. The densities of the crust and the subterranean mantle are assumed to be 2.67 and 3.27 gm/cm³ respectively. All the geophysical and geodetic quantities mentioned above can be obtained in a form of matrix products $Y_{ab}=\sum_i\sum_j X_{ij}\cdot\phi_{a-i,b-j}$ where $\phi_{a-i,b-j}$ is a response function to convert the given data X_{ij} (gravity anomaly or elevation) into Y_{ab}.

Section II consists of two-dimensional analyses carried out for three profile sections: the Canadian Shield, the Transcontinental section from the Pacific to the Atlantic coast, and the Cordillera. The grid interval for the gravity and elevation data has a range varying from 51.5 km to 210 km for these three sections, and thus the local variations of gravity and elevation with wave-lengths shorter than twice the grid interval (103 to 420 km) play no important part in the results. Section III is the three-dimensional analysis for the rectangular area bounded by longitudes 90° and 113°W and latitudes 49° and 62°N of Western Canada. The grid interval is 72 km and the total number of grid points for the Bouguer gravity anomaly is 21 × 21. To obtain the response functions ϕ_{ij} and matrix products $Y_{ab}=\sum_i\sum_j X_{ij}\cdot\phi_{a-i,b-j}$ numerical calculations were carried out using a digital computer.

A brief interpretation of the results is presented. The average crustal thicknesses which are derived from the condition Σ (isostatic gravity anomaly)^2 = minimum, were found to be 36.4 km and 48 km for the Canadian Shield and the southern Cordillera respectively. The Cordillera and Shield regions are isostatically over-compensated while for the central Prairie regions the opposite condition is true. In the area where the three-dimensional analysis is carried out the isostatic gravity anomalies range from −30 mgals in the north, to +20 mgals in the south. The deflections of the vertical do not exceed 4 seconds in the whole area with corresponding undulations of the geoidal heights varying from +5 m in the south to −8 m in the north. The effect of the Mesozoic or younger sediments near the surface of the Prairie region upon the over-all gravity field appear to be negligible.

RÉSUMÉ—A l'aide des anomalies de Bouguer et des élévations correspondantes de la surface au pays, l'auteur a pu étudier l'état physique de la croûte terrestre, la répartition des anomalies isostatiques, les ondulations de la limite croûte-manteau, les déviations de la verticale et les ondulations des hauteurs du géoïde. L'auteur utilise pour cette étude une modification du procédé de Tsuboi qui présuppose qu'une variation de la gravité est attribuable à des répartitions anormales de la masse à la base de la croûte. La partie I décrit les méthodes de calcul. L'auteur a évalué à 2.67 et 3.27 gm/cm³ respectivement les densités de la croûte et du manteau sous-jacent. Toutes les données géophysiques et géodésiques mentionnées ci-dessus peuvent être obtenues sous forme de produits matriciels $Y_{ab}=\sum_i\sum_j X_{ij}\cdot\phi_{a-i,b-j}$ où $\phi_{a-i,b-j}$ est une fonction de réponse servant à convertir X_{ij} (anomalie de gravité ou élévation) en Y_{ab}.

La partie II est composée d'analyses bi-dimensionnelles effectuées pour trois sections de profils: le bouclier canadien, la section transcontinentale, qui va du Pacifique à l'Atlantique, et la Cordillère. L'intervalle du quadrillage établi pour recueillir les données gravimétriques et altimétriques dans ces trois sections varie de 51.5 à 210 kilomètres de sorte que les variations locales de la gravité et de l'élévation qui ont des longueurs d'onde inférieures au double des intervalles du quadrillage (103 et 420 kilomètres) n'influent à peu près pas sur les résultats. La partie III est une analyse tri-dimensionnelle de la région rectangulaire bornée par les méridiens 90° et 113° ouest et les parallèles 49° et 62° nord. L'intervalle du quadrillage est de 72 kilomètres et le nombre total de stations nécessaires à l'établissement de l'anomalie gravimétrique de Bouguer est de 21 sur 21. Pour obtenir les fonctions de réponse ϕ_{ij} et les produits matriciels $Y_{ab}=\sum_i\sum_j X_{ij}\cdot\phi_{a-i,b-j}$ les calculs numériques ont été exécutés à l'aide d'une calculatrice arithmétique.

Les résultats sont brièvement interprétés. Les épaisseurs moyennes de la croûte qui sont dérivées de la condition: Σ (anomalie de gravité isostatique)^2 = minimum, étaient de 36.4 et de 48 kilomètres respectivement pour le bouclier canadien et la Cordillère méridionale. Du point de vue isostatique, les régions de la Cordillère et du Bouclier sont surcompensées tandis que c'est le contraire qui se produit dans le centre des Prairies. Dans la région où l'on a effectué une analyse tri-dimensionnelle, les anomalies de gravité isostatiques se sont échelonnées entre −30 milligals, au nord et +20 milligals au sud. Les déviations de la verticale ne dépassent pas 4 secondes dans toute la région, les ondulations correspondantes des élévations du géoïde variant de +5 mètres au sud à −8 mètres au nord. Dans la région des Prairies, les sédiments mésozoïques, ou plus récents, qui sont situés à proximité de la surface ne semblent avoir qu'un effet négligeable sur le champ de la gravité.

55560-7—2

INTRODUCTION

One of the important uses of gravity observations is their contribution to understanding the geophysical state of the crust. They provide information concerning the degree of isostatic equilibrium, the distribution of anomalous masses within and beneath the crust, and the undulation of the boundary separating the crust from the subterranean mantle. Gravity data corrected for heights and masses above sea level are compared with the values expected for a uniform earth. The discrepancy is called the Bouguer gravity anomaly and is suitable for structural studies since it is caused by anomalous mass distributions within and/or beneath the crust. Such mass distributions will be due in part to horizontal and vertical variations in density of the rocks composing the crust. Undoubtedly local anomalies within a restricted area are related to the surface geology, but the anomalies of large horizontal scale are most likely related to the major structure of the crust.

The over-all structure of the crust in Canada as inferred from the Bouguer gravity anomalies is discussed in this paper. It is assumed that the major variations in the gravity field reflect mass distributions due to undulations of the surface between the crust and mantle. In the present study the density of the crust and mantle are assumed to be uniform, 2.67 and 3.27 gm/cm^3 respectively, and all variations in the Bouguer gravity anomalies are due to changing crustal thicknesses. Thus an abnormally negative gravity field reflects an abnormally thick crust; for positive fields the reverse condition is true.

Analysis of gravity data also provides important geodetic information such as the variation in heights of the geoidal surface and the corresponding deflections of the vertical. It may be explained that the shape of the earth is defined essentially by the geoid which is that particular equipotential surface due to the earth's attraction and rotation, which corresponds to the mean sea-level surface. It is well known that the mean figure of the geoid is represented very closely by an oblate spheroid whose shorter axis coincides with the rotation axis of the earth. The geoid rises and falls according to the distributions of anomalous masses underneath the surface of the crust; it lies partly above and partly below the spheroid and the extent of the divergence is probably never greater than a hundred metres. The direction of gravity is perpendicular to the geoidal surface, and the angle between this direction and the normal to the spheroid is called the deflection of the vertical. Since both the height of the geoidal surface and deflections of the vertical depend upon mass distributions within or below the crust, they may be determined by analysis of the gravity field.

This investigation consists of two parts. Firstly, the computational methods outlined in Section I are applied in Section II in a two-dimensional analysis of three areas considered to represent the general features of the crust in Canada. These are, a transcontinental zone about latitude 50°, a section across the southern Canadian Cordillera and a section lying entirely within the Precambrian Shield (Figure 1).

Secondly, Section III gives a three-dimensional analysis of a rectangular area covering some 900 × 900 square miles in Western Canada. This area is bounded by latitudes 90° and 113°W and by latitudes 49° and 62°N.

The Bouguer gravity anomaly map of Canada provides the basic information for this study. This map is a compilation of some 10,000 regional measurements carried out at intervals of about 8 miles in Southern Canada and 10 to 15 miles in the northern regions. While the gravity data are believed consistent to better than 0.3 mgals, the greatest uncertainties result from poor elevation control—particularly in northern sections where errors as great as 5 m have been estimated (Innes and Thompson, 1953) for stations measured barometrically.

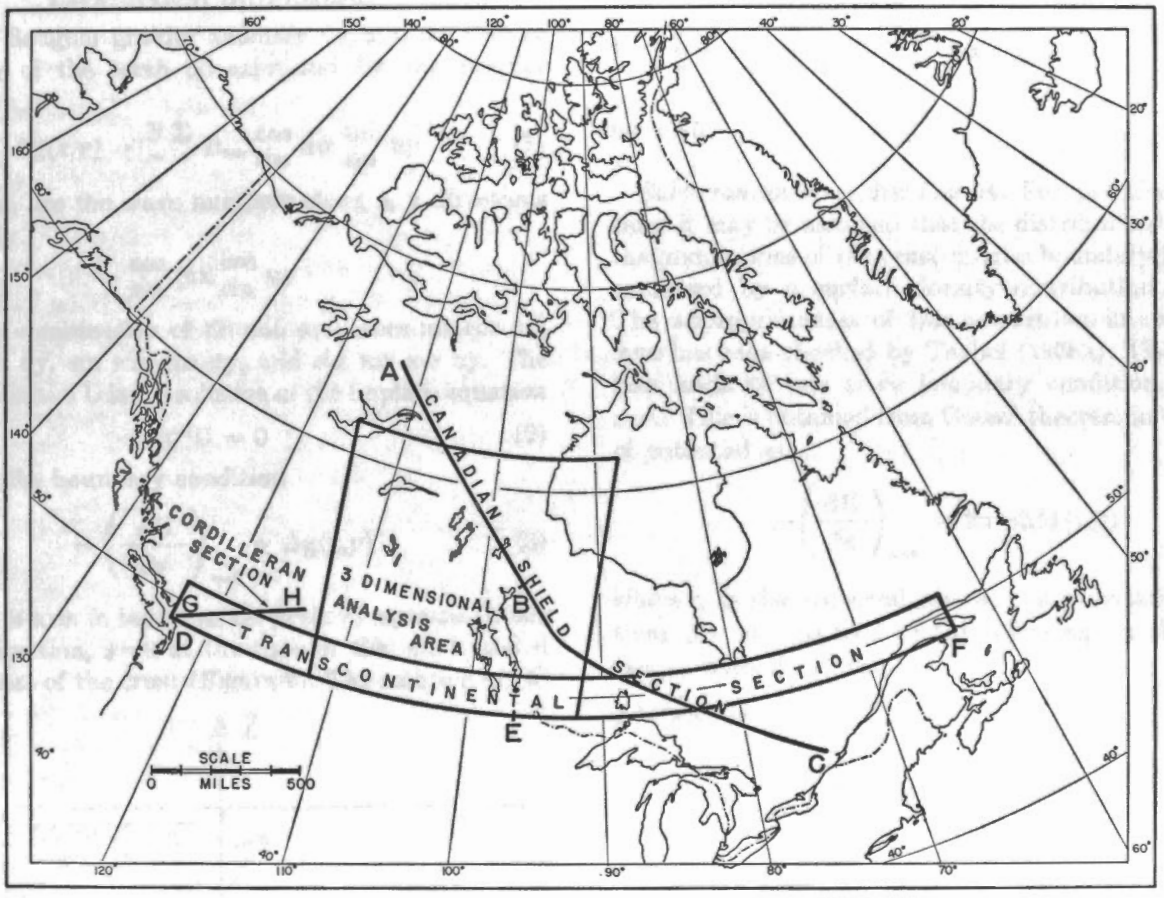

Figure 1. Location map showing areas of investigations.

SECTION I

METHOD OF ANALYSIS

Tsuboi (1937, 1938, 1939, 1940, 1942, 1949, 1950) developed a simple method by which it is possible to estimate from a gravity anomaly field, the corresponding subterranean mass distribution. The method assumes that the surface of the earth is a plane and that any variation in gravity is caused by the mass distributions at the base of the crust or by undulations of the boundary surface between the crust and the subterranean mantle.

Geophysical Implication

Let the Bouguer gravity anomaly $\Delta g(x,y)$ on a plane surface xy of the earth be expressed by the Fourier series as

$$\Delta g(x,y) = \sum_m \sum_n B_{mn} \begin{matrix}\cos\\ \sin\end{matrix} mx \begin{matrix}\cos\\ \sin\end{matrix} ny \qquad (1)$$

where m, n, are the wave numbers along x, y directions respectively.

$$\begin{matrix}\cos\\ \sin\end{matrix} mx \begin{matrix}\cos\\ \sin\end{matrix} ny$$

means any combination of sin and cos as cos mx cos ny, cos mx sin ny, sin mx cos ny, and sin mx sin ny. The gravity potential U is the solution of the Laplace equation

$$\nabla^2 U = 0 \qquad (2)$$

subject to the boundary condition

$$-\left(\frac{\partial U}{\partial z}\right)_{z=d} = \Delta g(x,y) \qquad (3)$$

where the z-axis is taken to be positive upward in the vertical direction, $z=0$ at the base of the crust, and d the thickness of the crust (Figure 2). The solution of (2)

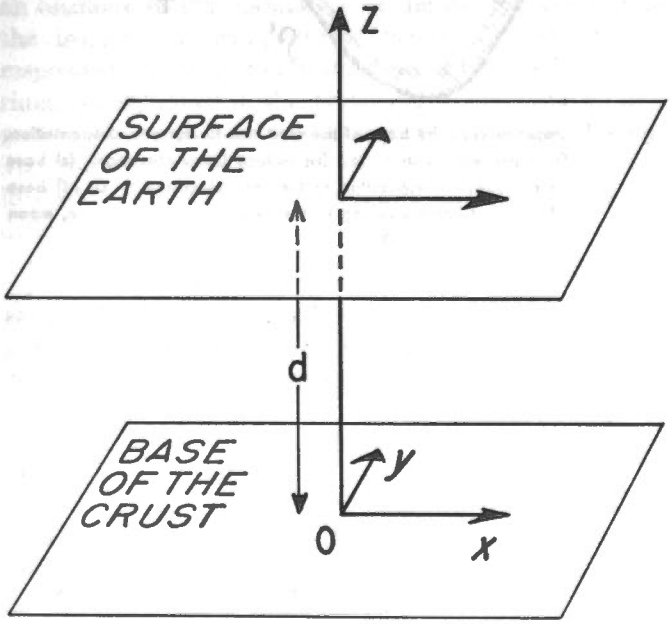

Figure 2. Coordinate system used in the investigation.

in the Cartesian coordinate system has the form

$$U = \sum_m \sum_n A_{mn} \begin{matrix}\cos\\ \sin\end{matrix} mx \begin{matrix}\cos\\ \sin\end{matrix} ny\, e^{-\sqrt{m^2+n^2}\, z} \qquad (4)$$

for the region $z>0$. Thus condition (3) indicates

$$\sqrt{m^2+n^2}\, A_{mn}\, e^{-\sqrt{m^2+n^2}\, d} = B_{mn}$$

or (5)

$$U = \sum_m \sum_n \frac{B_{mn}}{\sqrt{m^2+n^2}} \begin{matrix}\cos\\ \sin\end{matrix} mx \begin{matrix}\cos\\ \sin\end{matrix} ny\, e^{-\sqrt{m^2+n^2}\,(z-d)} \qquad (5)$$

for $z>0$.

Subterranean mass distribution: For practical applications it may be assumed that the distribution caused by the undulations of the crust-mantle boundary is suitably expressed by a surface density distribution $\Delta M(x,y)$. The appropriateness of this assumption in actual problems has been checked by Tsuboi (1938a). This assumption leads to one more boundary condition for U at $z=0$. This is obtained from Gauss' theorem in the theory of potential as

$$-\left(\frac{\partial U}{\partial z}\right)_{z=0} = 2\pi\gamma\Delta M(x,y) \qquad (6)$$

where γ is the universal constant of gravitation. Equations (5) and (6) lead to the following for the subterranean mass distribution:

$$\Delta M(x,y) = \qquad (7)$$

$$= \frac{1}{2\pi\gamma} \sum_m \sum_n B_{mn} \begin{matrix}\cos\\ \sin\end{matrix} mx \begin{matrix}\cos\\ \sin\end{matrix} ny\, e^{\sqrt{m^2+n^2}\, d}$$

A negative value for $\Delta M(x,y)$ would mean a mass deficiency at the base of the crust.

Boundary relief: The relief of the base of the crust $h(x,y)$ which is the deviation from the mean base of the crust may be expressed by

$$h(x,y) = \frac{\Delta M(x,y)}{\rho' - \rho} \qquad (8)$$

where ρ and ρ' are the densities of the materials composing the crust and the subterranean mantle respectively. They are assumed to be constant, 2.67 and 3.27 gm/cm^3 respectively. h(xy) is positive downward. Thus equation (8) shows that for areas underlain by mass deficiencies the crust is thicker than the average value d (Figure 3).

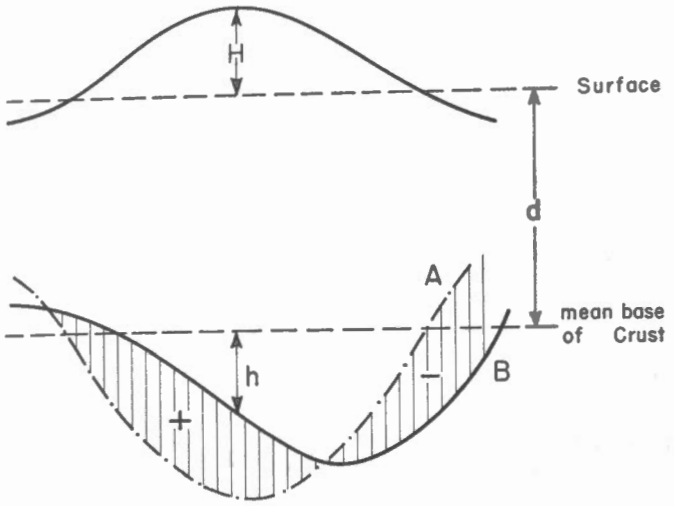

Figure 3. Isostatic equilibrium state and isostatic mass anomalies illustrated schematically for the two-dimensional case. d: mean crustal thickness; H: elevation; A: relief at base of crust for perfect isostatic equilibrium: B: relief at base of crust inferred from the Bouguer gravity anomaly, h, being the deviation from the mean base of the crust. Shaded area indicates a mass excess (+) or defect (−) compared to the perfect isostatic state.

Isostatic gravity anomaly: Let the surface elevation H(x,y) above sea level be expressed by

$$H(x,y) = \sum_m \sum_n H_{mn} \begin{matrix}\cos\\ \sin\end{matrix} mx \begin{matrix}\cos\\ \sin\end{matrix} ny \qquad (9)$$

The mass of the crust above sea level should be $\rho\, H(x,y)$ per unit area. The idea of Airy's hypothesis on isostasy implies that the negative of this mass, viz:

$$\Delta M'(x,y) = -\rho H(x,y) = \qquad (10)$$

$$= -\rho \sum_m \sum_n H_{mn} \begin{matrix}\cos\\ \sin\end{matrix} mx \begin{matrix}\cos\\ \sin\end{matrix} ny$$

is distributed at the base of the crust ($z=0$ plane) so as to exactly compensate the surface irregularities. Thus in continental sectors there is a downward undulation of the base of the crust beneath mountains, and in oceanic regions an upward undulation beneath ocean basins. The attraction at the surface of the earth due to the mass expressed in (10) is given by

$$\Delta g'(x,y) =$$

$$= -2\pi\gamma\rho \sum_m \sum_n H_{mn} \begin{matrix}\cos\\ \sin\end{matrix} mx \begin{matrix}\cos\\ \sin\end{matrix} ny\, e^{-\sqrt{m^2+n^2}\, d} \qquad (11)$$

which bears the same relation to (10) as (7) does to (1).

The isostatic gravity anomaly defined by:

$$\Delta g_{iso} = \Delta g - \Delta g'$$

$$= \Delta g + 2\pi\gamma\rho \sum_m \sum_n H_{mn} \begin{matrix}\cos\\ \sin\end{matrix} mx \begin{matrix}\cos\\ \sin\end{matrix} ny\, e^{-\sqrt{m^2+n^2}\, d} \qquad (12)$$

can be evaluated readily.

Isostatic mass anomaly: The isostatic mass anomaly is the excess or deficiency of mass at the base of the crust which gives rise to the isostatic gravity anomaly. It may be defined as follows:

$$\Delta M_{iso} = \Delta M - \Delta M' \qquad (13)$$

$$= \frac{1}{2\pi\gamma} \sum_m \sum_n B_{mn} \begin{matrix}\cos\\ \sin\end{matrix} mx \begin{matrix}\cos\\ \sin\end{matrix} ny\, e^{\sqrt{m^2+n^2}\, d} + \rho H(x,y)$$

The concepts developed above are illustrated in Figures 3 and 4. Profile A represents the relief at the base of the crust for a condition of perfect isostasy, while profile B is the relief inferred from the Bouguer gravity field. The difference shown by the shaded portion represents the isostatic mass anomaly given by equation (13).

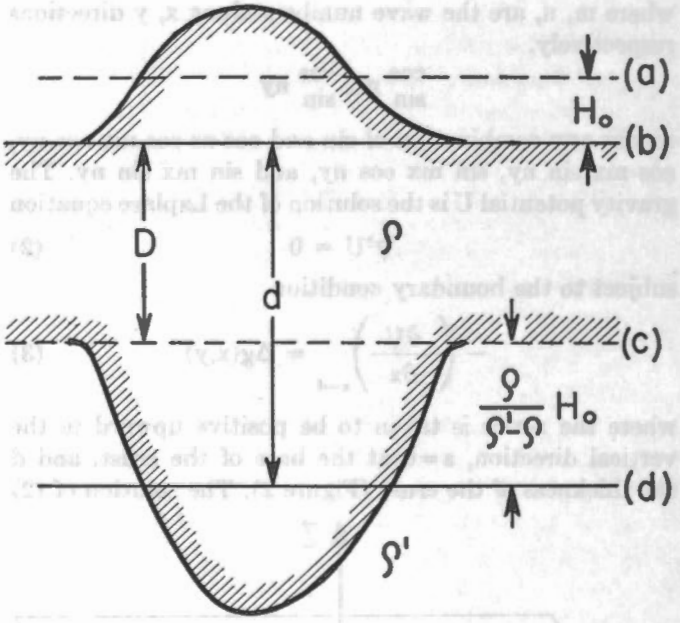

Figure 4. Depression of the base of the crust due to isostatic compensation. (a) mean elevation = H_0; (b) surface (zero elevation); (c) base of the crust corresponding to the zero elevation = D; (d) base of the crust corresponding to the mean elevation H_0 = d, mean depression = d − D.

It may be noted that the value d is the mean thickness of an actual crust having an average elevation H_{00} within the area. Thus the mean depression of the crust for this region is given by,

$$d - D = \frac{\rho}{\rho' - \rho} H_{00} \qquad (14)$$

where D is the thickness of the crust for an area of zero elevation and corresponds to the crustal thickness assumed in the Airy-Heiskanen method of isostatic reduction.

Over areas limited in extent the earth's surface may be approximated by a plane. On such an assumption it may be stated that a gravity anomaly interpreted by Airy's hypothesis and assuming a crustal thickness D, may also be interpreted by Pratt's hypothesis assuming a depth of compensation 2D, or exactly twice the thickness of the crust inferred from the Airy hypothesis (Tsuboi, 1954a). Thus any preceding discussion based upon Airy's hypothesis is equally applicable to the Pratt method. It is impossible to decide from the gravity data alone which is the more reasonable hypothesis.

The vertical gradient of gravity: The vertical gradient of gravity

$$\frac{\partial g}{\partial z}$$

at the surface of the earth, is used for the free air reduction of gravity data and is usually taken to be -3086×10^{-4} mgal./m. This value, however, is not constant but varies from place to place, depending upon the mass distribution within and beneath the crust, (Tsuboi, 1954b). The anomaly in the vertical gradient corresponding to the mass distribution expressed in equation (7) is given by:

$$\Delta\left(\frac{\partial g}{\partial z}\right)_{z=d} = \left(\frac{\partial \Delta g}{\partial z}\right)_{z=d} = -\left(\frac{\partial^2 U}{\partial z^2}\right)_{z=d}$$

$$= -\sum_m \sum_n \sqrt{m^2+n^2}\, B_{mn} \begin{matrix}\cos\\ \sin\end{matrix} mx \begin{matrix}\cos\\ \sin\end{matrix} ny \qquad (15)$$

Geodetic Implications

Now that the distribution of the isostatic gravity anomaly has been determined, it is not difficult to obtain an estimate of the undulation of the natural geoid from the isostatic or compensated geoid. The latter corresponds to a crustal condition of perfect isostatic equilibrium. As explained in the preceding section the natural geoid is that particular equipotential surface corresponding to the sea-level surface and its departure from the isostatic geoid is caused by the isostatic mass anomalies defined in equation (13).

The isostatic geoid* in this discussion becomes our reference surface which as previously explained is approximated by a plane.

Deflections of the vertical: The potential U′ along the surface of the earth corresponding to the isostatic gravity anomaly Δg_{iso} can be written as

$$U' = \sum_m \sum_n \frac{(\Delta g_{iso})_{mn}}{\sqrt{m^2+n^2}} \begin{matrix}\cos\\ \sin\end{matrix} mx \begin{matrix}\cos\\ \sin\end{matrix} ny \qquad (16)$$

from (5) where $(\Delta g_{iso})mn$ is the Fourier component of Δg_{iso}. The direction of gravity is everywhere normal to the natural geoid (*see* Figure 5). The deflections of the

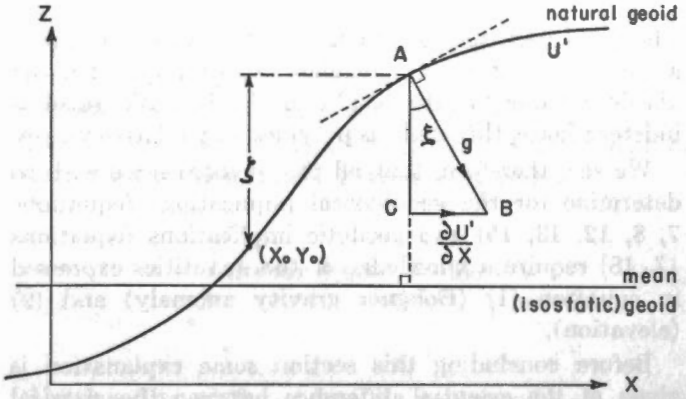

Figure 5. Schematic diagram to illustrate geoidal height ζ relative to an arbitrarily selected reference point X_0Y_0, and the component of the deflection of the vertical ξ taken along the X axis. AB = − g (inward direction of gravity);

$$CB = \frac{\partial U'}{\partial x}, \quad \xi \doteq \sin \xi = \frac{1}{g}\frac{\partial U'}{\partial x}.$$

vertical which are defined by the angle between this direction and the normal to the reference surface, horizontal plane in this case, are obtained for the x and y directions from the following equations:

$$\xi = -\frac{1}{g}\left(\frac{\partial U'}{\partial x}\right)_{z=d} =$$

$$-\frac{1}{g}\sum_m \sum_n \frac{m}{\sqrt{m^2+n^2}} \times (\Delta g_{iso})_{mn} \begin{matrix}\sin\\ \cos\end{matrix} mx \begin{matrix}\cos\\ \sin\end{matrix} ny \qquad (17)$$

$$\eta = -\frac{1}{g}\left(\frac{\partial U'}{\partial y}\right)_{z=d} =$$

$$-\frac{1}{g}\sum_m \sum_n \frac{n}{\sqrt{m^2+n^2}} \times (\Delta g_{iso})_{mn} \begin{matrix}\cos\\ \sin\end{matrix} mx \begin{matrix}\sin\\ \cos\end{matrix} ny$$

As a result of the particular choice of the co-ordinate system, here ξ and η designate the components of the deflections in the direction of the prime vertical and the meridian respectively. This contrasts with the conventional nomenclature in geodesy where ξ and η are used to designate the meridinal and prime vertical components respectively.

For practical application it is sufficient to use a mean value of g = 980 c.g.s.

*Usually the undulation of the geoid is measured from the niveau spheroid which corresponds to the normal gravity formula used for deriving the gravity anomalies. In the present case, from the nature of the theory on which the present calculations are based, it is evident that the undulation of the geoid should be measured from a geometrical horizontal plane. If the perfect isostatic equilibrium state is assumed within the area with which we are concerned, the geoid corresponding to this average state will be approximated by a plane. It may be referred to as the mean (isostatic) geoid.

Undulations of the geoid: The height of the geoid at x, y relative to an arbitrary point x_o, y_o (see Figure 5) is given by

$$\zeta(x,y) = \frac{1}{g} \sum_m \sum_n \left[\frac{(\Delta g_{iso})_{mn}}{\sqrt{m^2 + n^2}} \left\{ \begin{matrix} \cos \\ \sin \end{matrix} mx \begin{matrix} \cos \\ \sin \end{matrix} ny - \begin{matrix} \cos \\ \sin \end{matrix} mx_o \begin{matrix} \cos \\ \sin \end{matrix} ny_o \right\} \right] \tag{18}$$

The geoid rises and falls in areas with positive and negative isostatic gravity anomalies respectively. Since the absolute value for the height of the isostatic geoid is indeterminate, this analysis provides only relative values.

We see, therefore, that all the quantities we wish to determine for the geophysical implications (equations 7, 8, 12, 13, 15) and geodetic implications (equations 17, 18) require a knowledge of the quantities expressed in equation (1) (Bouguer gravity anomaly) and (9) (elevation).

Before concluding this section some explanation is given of the essential difference between the classical methods of Airy-Heiskanen and Pratt-Hayford and the method used here in calculating the isostatic gravity anomaly. The former methods give the value of the isostatic anomaly at each particular station and include the contributions from the whole crust of the earth. The latter gives only the general trend of the anomaly within a limited area, and includes only the contribution from that area. It is true that in some cases the exact and absolute values of the anomaly at the respective stations are needed. However, for many geophysical studies only the general feature of the isostatic gravity anomaly field is required and the present method is adequate. Since gravity is the normal derivative of the potential, the contribution from mass distributions not directly below the station will be small. It follows, therefore, that the present method should provide fairly accurate results for the isostatic gravity anomaly or isostatic mass anomaly although only contributions from the limited area are concerned.

Several methods are known for deducing the undulation of the geoid and the deflections of the vertical from gravity anomalies. In the well-known method of Stokes (1849), it is necessary that the gravity anomaly field over the whole surface of the earth be known with sufficient density to permit a spherical harmonic expansion of its distribution. The methods of Pizetti (1911), Vening Meinesz (1928), and Heiskanen (1957) have their origin in the method of Stokes, and have been devised to make the calculations involved more practicable. In these methods, it is necessary to extend the integration over the whole surface of the earth.

In the present method only a rectangular portion of the earth's surface is considered and this is assumed to be a plane surface. It is further assumed that the gravity anomaly is repeated periodically in directions that are perpendicular to the sides of the rectangular area. The method was originally developed by Tsuboi (1937 to 1950) who calculated the deflections of the vertical and the undulations of the geoidal heights for the United States and East Indies. Hayford (1909), in his classical work on isostasy, gave the deflections of the vertical in the United States, using Pratt's isostatic method of reduction. Vos van Steenwijk (1946), applied the method of Vening Meinesz to calculate the undulation of the geoid in the East Indies from the gravity field. Tsuboi's results show sufficient agreement with these calculations. We now see that, although in the present method almost no attention is paid to the contribution of the gravity anomaly outside the area in question, the results obtained are satisfactorily accurate for many geodetic purposes. This justifies its use for calculating the undulations of the geoid from gravity anomalies in many regions which otherwise would remain unknown until a great deal more data could be made available.

Although the present method provides only relative values of the deflections and geoidal heights, observations of these quantities by geodetic surveys have the same defect, since they cannot provide absolute values until an international reference system has been established and intercontinental connections completed. The practical application of the more precise methods (Rice, 1952 and Tsuboi, 1954a) applying gravity data to geodetic problems must await the establishment of many more stations throughout the world.

SECTION II

GEOPHYSICAL STUDY BY TWO-DIMENSIONAL ANALYSIS

Modified Method of Analysis

Though Tsuboi's method is very useful in solving many gravity problems, it requires tedious and painstaking effort to carry out the Fourier analyses (1) and (9) and syntheses (7), (11), (15), and (17), if the higher harmonics are to be included. Moreover the amplitudes of B_{mn} and H_{mn} are not of interest, but only the results of the syntheses. Tomoda and Aki (1955) have developed a modified method from which the mass distribution may be derived directly without computing the Fourier coefficients. For the two-dimensional case let $n=0$ and thus formula (7) becomes

$$\Delta M(x) = \frac{1}{2\pi\gamma} \sum_m B_m e^{md} \begin{matrix}\cos\\ \sin\end{matrix} mx \qquad (7a)$$

As stated previously it is desired to avoid calculation of the coefficients B_m.* This is possible by using the function

$$\frac{\sin x}{x}$$

which has unit value at $x=0$ and vanishes if $x=\alpha\pi$ where a is any positive or negative integer (*see* Figure 6). The

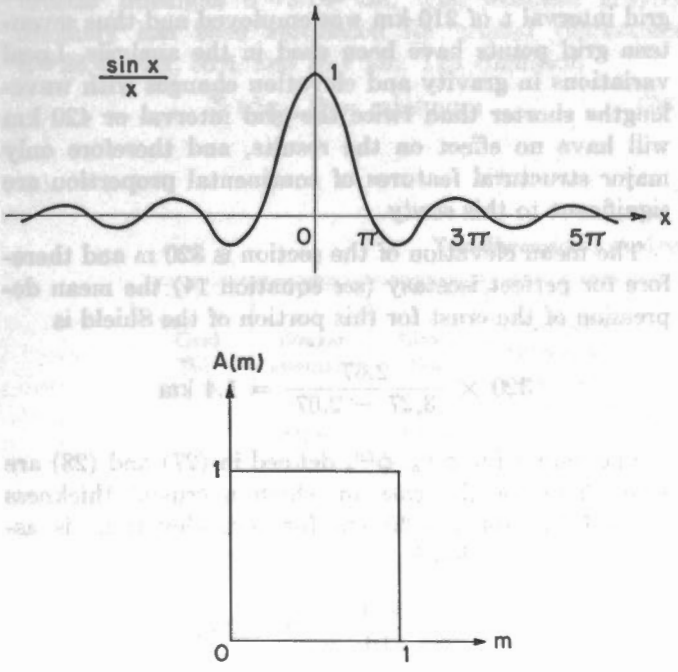

Figure 6. Plot of the function $\frac{\sin x}{x}$ and plot of its Fourier cosine transform A(m) for positive values of m.

Fourier cosine transform of this function is

$$A(m) = \frac{1}{2\pi}\int_{-\infty}^{\infty} \frac{\sin x}{x} \cos mx\, dx \begin{matrix} = 1 & |m| < 1 \\ = \frac{1}{2} \text{ if } & |m| = 1 \\ = 0 & |m| > 1 \end{matrix} \qquad (19)$$

The plot of this for positive arguments is shown in Figure 6. In these formulae m is the wave number (reciprocal of wave-length) and it may easily be seen that if $m>1$ then the wave-length is smaller than twice the grid distance. The transformation therefore eliminates the effect of the local variations of the gravity field. Since

$$\int_0^1 \cos mx\, dm = \frac{1}{x} \sin x \qquad (19a)$$

the mass $\tilde{\Delta m}$, at the grid points $x=a\pi$ and $z=0$, which causes the gravity

$$\tilde{\Delta g} = B(x = a\pi) \frac{\sin x}{x} \qquad (20)$$

at $x=a\pi$ and $z=d$ becomes

$$\tilde{\Delta M}\,(x = a\pi) = \frac{1}{2\pi\gamma} B(x = a\pi) \int_0^1 \cos ma\pi e^{md}\, dm. \qquad (21)$$

Since $\Delta g(x)$ along the earth's surface is the overlapping sum of

$$\tilde{\Delta g}(x)$$

with its origin appropriately displaced, it can be written as

$$\Delta g(x) = \sum_i B_i \frac{\sin (x - i\pi)}{i\pi} . \qquad (22)$$

The mass ΔM at $z=0$ which corresponds to Δg is given by

$$\Delta M = \frac{1}{2\pi\gamma} \sum_i B_i \int_0^1 \cos mi\pi e^{md}\, dm. \qquad (23)$$

In the above expressions x, z, d are in radians when the distance between the successive grid points is taken as π.

An extension of the above modified method to the problem of isostatic gravity anomaly is not difficult.

*For additional information on this subject, see any standard textbook on Fourier transforms, for example (i) Carslaw, H.S. (1930) *Fourier's series and Integrals.* (ii) Brillouin, L. *Science and information theory,* Academic Press Inc., N.Y. 1956; or Tsuboi, C. and Tomoda, Y. *The relation between the Fourier series method and the* $\frac{\sin x}{x}$ *method for gravity interpretations.* J. Phys. Earth, v. 6, no. 1, 1958.

The result can be reduced to evaluating the overlapping sum

$$\Delta g' = -2\pi\gamma\rho \sum_i H_i \int_0^1 \cos mi\pi e^{-md}\, dm. \quad (24)$$

The integrals in (23) and (24) can easily be evaluated. The final results are obtained as follows

$$\Delta M(a) = \frac{1}{2\pi\gamma} \sum_i B_i \phi^{(1)}_{a-i} \quad (25)$$

$$\Delta g'(a) = -2\pi\gamma\rho \sum_i H_i \phi^{(2)}_{a-i} \quad (26)$$

where

$$\phi^{(1)}_a = \frac{c}{\pi(a^2 + c^2)} \left[\pm e^{c\pi} - 1 \right] \quad \begin{matrix} a \text{ even} \\ \text{odd} \end{matrix} \quad (27)$$

$$\phi^{(2)}_a = -\frac{c}{\pi(a^2 + c^2)} \left[\pm e^{-c\pi} - 1 \right] \quad \begin{matrix} a \text{ even} \\ \text{odd} \end{matrix} \quad (28)$$

and a is any integer defined by $x = a\pi$. The ratio of the thickness of the crust to the grid interval is given by

$$c = \frac{d}{L}$$

where L is the interval between successive points along the x-axis. The actual evaluation by overlapping summations gives

$$\begin{aligned} \Delta M(0) &= 2.386 \times 10^3 [\ldots\ldots + B_{-1}\phi^{(1)}_{-1} + \\ &\qquad B_0\phi^{(1)}_0 + B_1\phi^{(1)}_1 + \ldots\ldots] \\ \Delta M(1) &= 2.386 \times 10^3 [\ldots\ldots + B_{-1}\phi^{(1)}_{-2} \\ &\qquad + B_0\phi^{(1)}_{-1} + B_1\phi^{(1)}_0 + \ldots\ldots] \end{aligned} \quad (29)$$

(in units of gr/cm²)

$$\begin{aligned} \Delta g'(0) &= -11.19 [\ldots\ldots + H_{-1}\phi^{(2)}_{-1} + \\ &\qquad H_0\phi^{(2)}_0 + H_1\phi^{(2)}_1 + \ldots\ldots] \\ \Delta g'(1) &= -11.19 [\ldots\ldots + H_{-1}\phi^{(2)}_{-2} \\ &\qquad + H_0\phi^{(2)}_{-1} + H_1\phi^{(2)}_0 + \ldots\ldots] \end{aligned} \quad (30)$$

(in units of mgals).

with B in milligals and H in metres. Some properties of the integrals $\phi^{(1)}_a$, $\phi^{(2)}_a$ may be noted as follows:

symmetry

$$\begin{aligned} \phi^{(1)}_a &= \phi^{(1)}_{-a} \\ \phi^{(2)}_a &= \phi^{(2)}_{-a}, \end{aligned} \quad (31)$$

convergency

$$\begin{aligned} \sum_{a=-\infty}^{\infty} \phi^{(1)}_a &= 1 \\ \sum_{a=-\infty}^{\infty} \phi^{(2)}_a &= 1. \end{aligned} \quad (32)$$

Since observational data for B_a and H_a cannot cover an infinite section from $a = -\infty$ to $+\infty$, it is assumed that $B = 0$ and $H = 0$ for the region with values of a beyond the region where the observed data are available. Then it can easily be seen that ΔM and $\Delta g'$ for the grid points near the ends of the section line are inaccurate.

The following quantities are readily obtained:

Isostatic gravity anomaly

$$\Delta g_{iso}(a) = B(a) - \Delta g'(a), \quad (33)$$

isostatic mass anomaly

$$\Delta M_{iso}(a) = \Delta M(a) + \rho H(a), \quad (34)$$

undulation of the relief base of the crust

$$h(a) = \frac{\Delta M}{\rho' - \rho} = 39.76 \times 10^{-2} \sum_i Bi\, \phi^{(0)}_{a-i}. \quad (35)$$

(in units of km).

The Canadian Shield Section

A study of the geophysical state of the Canadian Shield is of special interest. The section selected for study (*see* Figure 1) includes two important geological provinces, the Churchill (A-B) and Superior (B-C) provinces, with a total length of about 3,400 km. The grid interval L of 210 km was employed and thus seventeen grid points have been used in the analysis. Local variations in gravity and elevation changes with wavelengths shorter than twice the grid interval or 420 km will have no effect on the results, and therefore only major structural features of continental proportion are significant to this study.

The mean elevation of the section is 320 m and therefore for perfect isostasy (*see* equation 14) the mean depression of the crust for this portion of the Shield is

$$320 \times \frac{2.67}{3{,}27 - 2.67} = 1.4 \text{ km}$$

The values for $\phi^{(1)}_a$, $\phi^{(2)}_a$ defined in (27) and (28) are given here for the case in which a crustal thickness $d = 36.4$ km (or $D = 35$ km for zero elevation) is assumed. For this depth

$$c = \frac{36.4}{210} = 0.17333,$$

and since a extends from -8 to $+8$ the following values are obtained:

a	$\phi^{(1)}_a$	$\phi^{(2)}_a$
0	1.30770	0.77108
±1	−0.13581	0.08464
±2	0.00869	0.00576
±3	−0.01544	0.00964

±4	0.00220	0.00143
±5	−0.00557	0.00347
±6	0.00098	0.00064
±7	−0.00283	0.00178
±8	0.00055	0.00035

Equation (32) provides a check on the accuracy of the numerical integration as follows:

$$\sum_{a=-8}^{8} \phi^{(1)}{}_a = 1.01324$$

$$\sum_{a=-8}^{8} \phi^{(2)}{}_a = .98650$$

These results lie within 1.3 and 1.4 per cent respectively of the limiting value and there is little to be gained by extending the analysis to include higher values of a. Moreover, all values obtained for ΔM and $\Delta g'$, except for grid points at each end of the section, have a reasonable accuracy.

The data used and results of the analysis are given in Table I. The mass distribution, isostatic mass anomaly, and the relief at the base of the crust are tabulated for a crustal thickness d = 36.4 km. The isostatic gravity anomaly has been calculated for crustal thicknesses d = 28.4, 34.4, 36.4, and 38.4 km. The condition

$$\Sigma (\Delta g_{iso})^2 = \text{minimum} \qquad (36)$$

suggests a crustal thickness of d = 36.4 km or D = 35 km for this region of the Canadian Shield (*see* Table II). This value is in good agreement with the depth of the Mohorovičić discontinuity determined by Hodgson (1953) from seismological studies in northern Ontario.

TABLE II

$\Sigma(\Delta g_{iso})^2$ for the Canadian Shield Section

d(km)	Zero elevation thickness D(km)	$\Sigma(\Delta g_{iso})^2$
28.4	27	4951.3
34.4	33	4574.2
36.4	35	4547.4
38.4	37	4650.6

In a comprehensive study of the implications of the gravity data in the Shield areas of Manitoba and Ontario, which partly overlap the region of this study, Innes (1960) deduced that the local gravity anomaly is intimately connected with the surface geology. However, the results obtained here are concerned chiefly with the undulation of the boundary layer at the base of the crust. It is quite apparent (*see* Figure 7) that there is a general trend of negative isostatic anomaly along the

TABLE I

Two-dimensional Analysis for the Canadian Shield Section

Grid No.	Bouger anomaly (mgals)	Elevation (metres)	Subterranean anomalous mass for d = 36.4 km (10^5gm/cm^2)	Isostatic Gravity Anomaly				Isostatic mass anomaly d = 36.4 km (10^5gm/cm^2)	Relief at base for d = 36.4 km (km)
				d = 28.4 D = 27	34.4 33 (mgals)	36.4 35	38.4 37		
−8	−59	399	−1.53	−20.8	−20.6	−20.3	−20.9	−0.46	−2.55
−7	−60	381	−1.41	−20.4	−19.7	−19.6	−20.5	−0.39	−2.34
−6	−61	357	−1.43	−23.4	−22.6	−22.6	−22.6	−0.48	−2.39
−5	−66	367	−1.55	−27.4	−26.6	−26.5	−26.6	−0.57	−2.59
−4	−66	381	−1.59	−26.8	−25.9	−25.9	−26.0	−0.57	−2.65
−3	−50	305	−1.13	−17.4	−16.6	−16.5	−16.8	−0.32	−1.89
−2	−44	263	−1.04	−16.1	−15.2	−15.2	−15.2	−0.34	−1.73
−1	−30	198	−0.64	− 7.5	− 6.6	− 6.7	− 6.6	−0.11	−1.06
0	−32	251	−0.73	− 4.8	− 3.9	− 4.0	− 3.9	−0.07	−1.15
1	−33	351	−0.71	3.4	4.0	4.2	3.8	0.23	−1.17
2	−54	366	−1.33	−16.2	−15.3	−15.3	−15.4	−0.36	−2.22
3	−44	314	−1.00	−10.9	−10.1	−10.1	−10.2	−0.16	−1.66
4	−42	259	−0.96	−13.6	−12.9	−12.8	−13.0	−0.26	−1.59
5	−50	314	−1.21	−18.0	−17.4	−17.4	−17.7	−0.38	−2.02
6	−39	244	−0.88	−12.8	−12.0	−12.0	−12.0	−0.23	−1.47
7	−42	259	−1.05	−17.0	−16.1	−16.0	−16.2	−0.35	−1.74
8	−20	91	−0.46	− 9.5	− 9.1	− 9.1	− 9.1	−0.21	−0.76

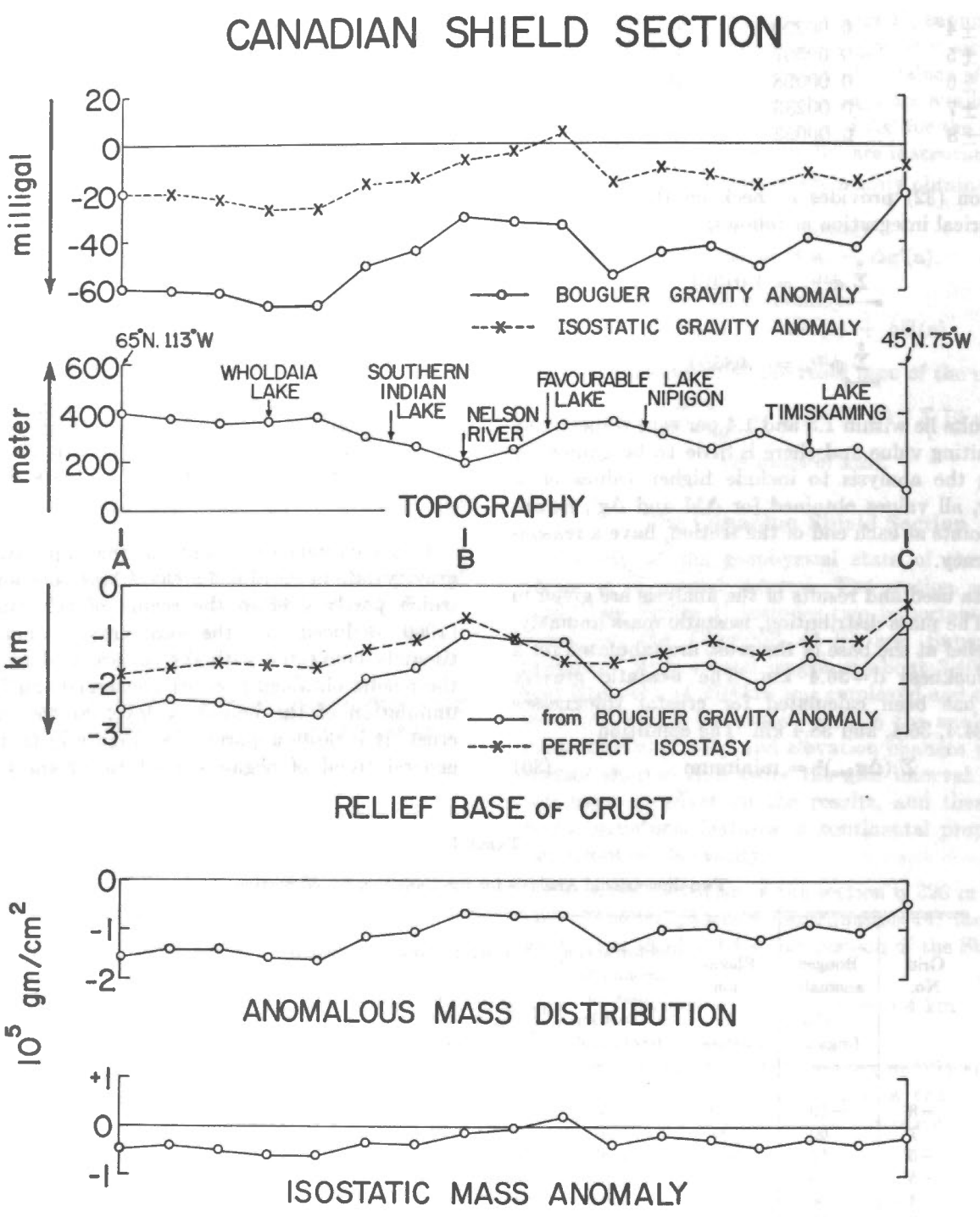

Figure 7. Two-dimensional analysis for the Canadian Shield section.

section, suggesting an over-compensated state, as Innes concluded.

It is well known that some rocks composing the Canadian Shield have densities considerably higher than average. Measurements (Thompson and Garland, 1957) and (Innes, 1960) show the Temiskaming-Keewatin volcanic sedimentary group and certain granite gneisses often extending over wide areas have densities of about 2.9 gm/cm², much heavier than generally assumed for crustal rocks. If isostatic compensation is perfect in the crust in this section, the mean density can be estimated from the relation

Mean Bouguer anomaly = $-2\pi\gamma\rho$ times mean elevation. (37)

Substitution of −46.5 mgal for the mean anomaly and 320 m for the mean elevation, the relation (37) gives the unreasonably high value of 3.48 gm/cm³. Thus it may be inferred that the crust beneath this region of the Shield is in a state of over-compensation in spite of the rather high density determined by surface sampling.

This interpretation of the anomalies suggests that the maximum undulation of the boundary layer at the base of the crust is in the vicinity of the Nelson River. This undulation has an amplitude of nearly 2 km or approximately 5 per cent of the thickness of the crust. The horizontal gradient amounts to about one part in six hundred.

Transcontinental Section

The transcontinental section (C—F, Figure 1) selected for study lies between latitudes 49 and 51°N and extends from the Pacific to the Atlantic coast. The gravity and elevation data are based upon mean values calculated for each square degree (1° × 1°) of longitude and latitude in the preparation of a Bouguer anomaly map of Canada. The values adopted for each grid point are indicated on Table III. For a grid point designated by longitude 111°W, for example, the values are based upon averages for the area bounded by latitudes 49° and 51°N and longitudes 110° and 112°W. The total length of the section is 4,200 km, involving thirty-one grid points with an interval of 140 km.

The mean elevation of this profile is 433 m and therefore according to equation (14) the mean depression of the crust is 1.93 km. In a previous investigation, Miller and Hughson (1936) determined the thickness of the crust using the condition (36) and gravity data based upon 128 pendulum determinations. Their stations lie within an east-west belt throughout Southern

TABLE III

Two-dimensional Analysis for the Transcontinental Section

Longitude	Bouguer anomaly (mgals)	Elevation (metres)	Subterranean anomalous mass (10^5gm/cm²)	Isostatic gravity anomaly (mgals)	Isostatic mass anomaly (10^5gm/cm²)	Relief at base (km)
123	− 27	24	−0.16	− 8.8	−0.09	−0.26
121	−129	884	−3.78	−43.3	−1.42	−6.30
119	−134	1008	−3.16	−22.4	−0.47	−5.27
117	−170	1505	−4.57	−20.4	−0.55	−7.61
115	−159	1398	−4.17	−15.3	−0.43	−6.32
113	−111	989	−2.61	1.5	0.03	−4.41
111	− 88	788	−2.11	0.1	0.00	−3.51
109	− 72	837	−1.64	17.7	0.59	−2.74
107	− 71	723	−1.81	8.8	0.12	−3.02
105	− 52	630	−1.17	18.4	0.51	−1.95
103	− 45	601	−1.04	20.5	0.57	−1.73
101	− 42	514	−1.10	14.2	0.28	−1.83
99	− 20	363	−0.29	22.2	0.68	−0.48
97	− 23	251	−0.53	9.4	0.14	−0.89
95	− 23	326	−0.45	13.9	0.42	−0.74
93	− 36	372	−0.86	5.3	0.15	−1.42
91	− 48	413	−1.32	− 4.6	−0.22	−2.20
89	− 35	323	−0.69	3.2	0.18	−1.15
87	− 47	319	−1.32	−13.5	−0.47	−2.21
85	− 29	203	−0.57	− 3.8	−0.03	−0.96
83	− 26	195	−0.59	− 3.0	−0.07	−0.99
81	− 27	206	−0.49	2.9	0.06	−0.82
79	− 51	259	−1.34	−22.5	−0.65	−2.23
77	− 59	270	−1.52	−27.9	−0.80	−2.53
75	− 55	365	−1.27	−16.4	−0.30	−2.12
73	− 68	382	−1.82	−26.9	−0.60	−3.04
71	− 57	422	−1.46	− 5.9	−0.33	−2.43
69	− 39	369	−0.84	1.2	0.14	−1.40
67	− 42	222	−1.19	−16.4	−0.60	−1.98
65	− 18	183	−0.38	0.6	0.11	−0.64
65	0	0	0.13	3.8	0.13	0.21

Canada about 350 miles wide, extending from Halifax to Victoria. Since this belt overlaps the transcontinental section under consideration, their value D = 35 km for the Airy hypothesis has been adopted for this study.

The results of the analysis are given also in Table III and illustrated in Figure 8. For the purposes of discussion the whole profile may be divided into three sections depending upon whether the isostatic anomalies are positive or negative. West of longitude 112°W the anomalies are negative and have a minimum value of −43 mgals. From 112° to 92°W the anomaly is positive, reaching a maximum of +22 mgals between Regina and Winnipeg. For the rest of the section to the east the anomalies are generally negative, having minimum values throughout south central Quebec.

The variation in the isostatic anomalies correlates to

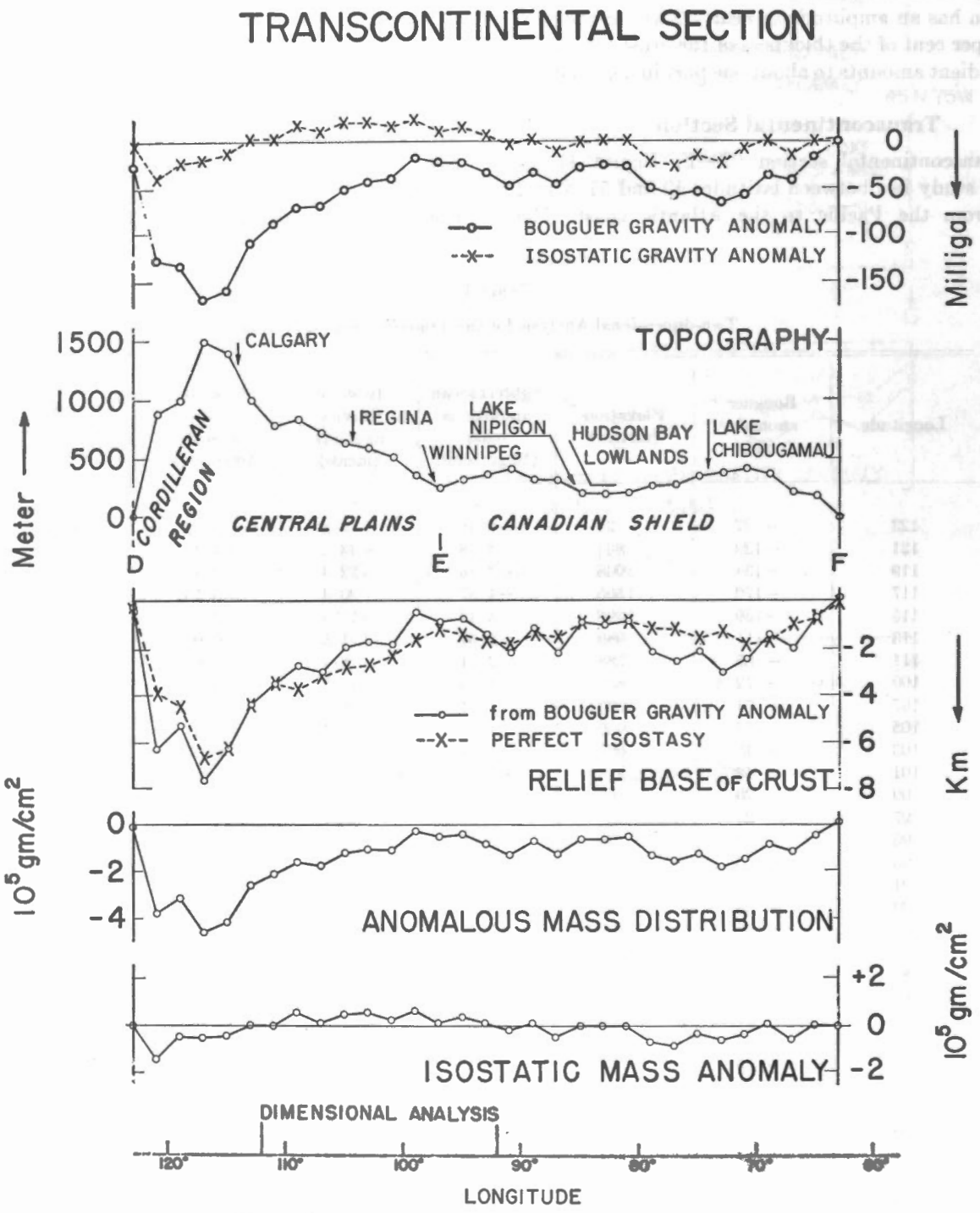

Figure 8. Two-dimensional analysis for the Transcontinental section.

some extent with the physiographic-geologic provinces. Generally the anomalies are negative over the Canadian Cordillera in the western part of the section and over the eastern part of the Precambrian Shield. On the other hand, the positive anomalies may be correlated with the great sedimentary basin of the Central Plains.

It is difficult to account for this correlation on the basis of the density variations in the crustal rocks of these contrasting areas. It has already been pointed out that rocks of the Precambrian Shield areas may be heavier than 2.67 gm/cm³. the density assumed in reducing the gravity data. Moreover, it is likely that the sedimentary rocks underlying the Central Plains region have somewhat lower densities than 2.67 gm/cm³. If this is so the effect would be to increase the amplitude of the gravity anomalies for these areas and thus make more difficult their explanation in terms of density variation within the crust.

This suggests that the isostatic anomaly may be largely due to undulations at the base of the crust which can be seen from relation (37). Assuming a perfect state of isostatic adjustment according to Airy's hypothesis, it is found that a density of 2.18 gm/cm³ is required to explain the mean positive anomaly over the Central Plains region. This value is much too small considering the fact that the results of borings within this area show the base of the sedimentary rocks, i.e. the Precambrian floor, lies at a depth of 6,000 feet (2 km) at most. This shows that the sedimentary layer of low density material has a thickness less than 10 per cent of the thickness adopted for the crust in this area.

It seems reasonable to conclude, therefore, that density

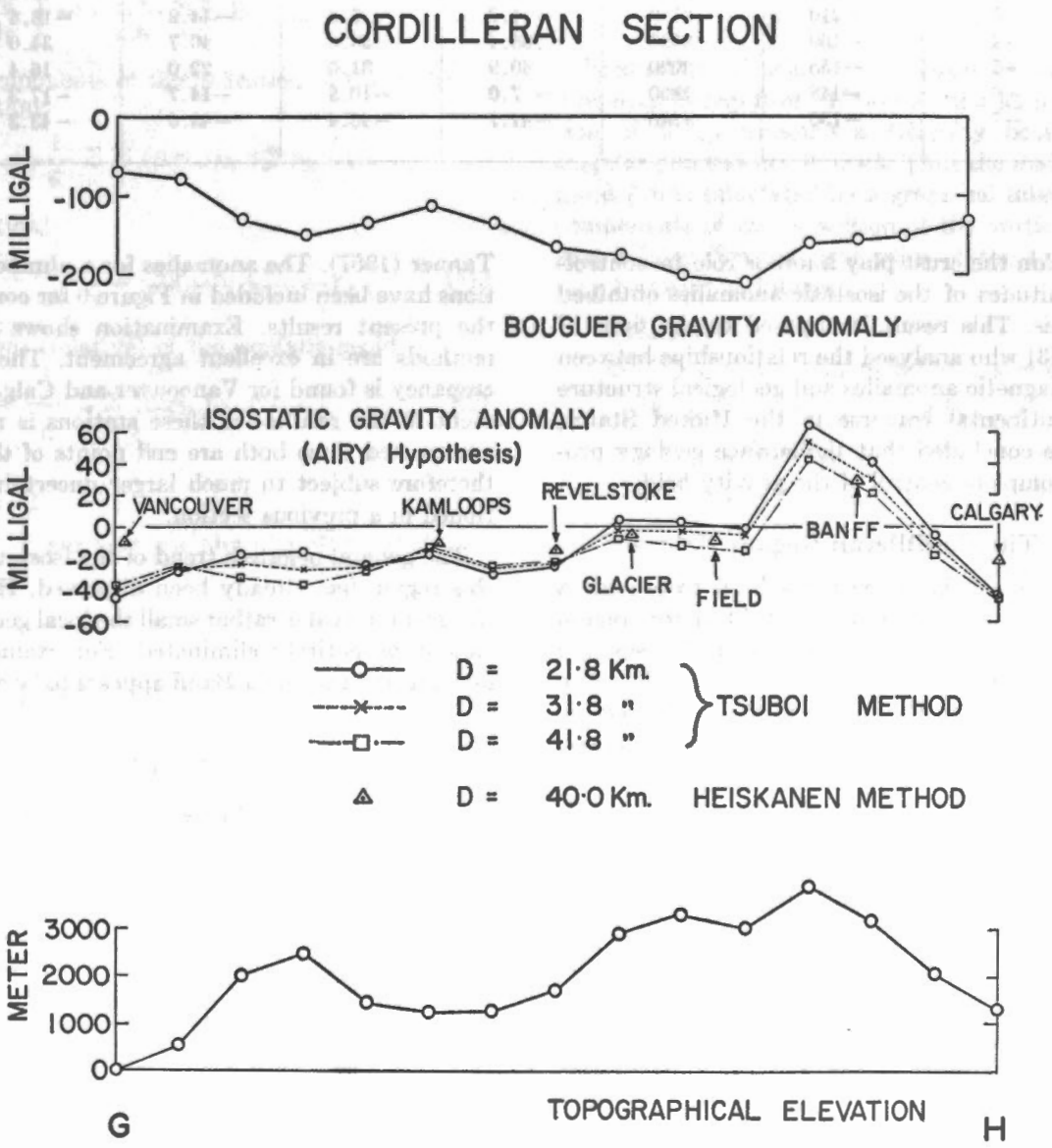

Figure 9. Two-dimensional analysis for the Cordilleran section.

TABLE IV

Two-dimensional Analysis for the Cordilleran Section

Grid No.	Bouguer anomaly (mgals)	Elevation (metres)	Isostatic Gravity Anomaly			
			d=30 km or D=21.8	d=40 km D=31.8 (mgals)	d=50 km D=41.8	d=56.5 km D=48.3
7	− 63	0	−44.8	−40.8	−37.7	−36.0
6	− 80	490	−27.2	−24.6	−24.8	−24.7
5	−129	1830	−18.0	−25.6	−32.0	−35.6
4	−152	2280	−17.6	−27.4	−35.5	−40.0
3	−134	1340	−23.9	−25.1	−26.7	−27.9
2	−115	1130	−16.9	−15.0	−13.7	−13.1
1	−134	1160	−29.7	−27.1	−25.2	−23.2
0	−155	1520	−23.6	−23.3	−22.6	−22.8
−1	−175	2650	5.1	− 1.5	− 7.4	−10.9
−2	−200	3010	4.8	− 3.6	−11.2	−15.8
−3	−210	2740	− 1.2	− 7.4	−14.2	−18.6
−4	−160	3590	65.4	53.0	40.7	34.0
−5	−155	2920	40.9	31.0	22.0	16.4
−6	−148	1890	− 7.0	−10.8	−14.7	−17.3
−7	−130	1240	−41.7	−42.4	−43.0	−43.3

variations within the crust play a minor role in controlling the magnitudes of the isostatic anomalies obtained in this analysis. This result is opposed to the finds of Woollard (1943) who analysed the relationships between gravity and magnetic anomalies and geological structure for a transcontinental traverse in the United States, from which he concluded that the surface geology provides nearly complete control of the gravity field.

The Cordilleran Region

A separate analysis has been carried out to provide a more detailed picture of the gravity field in this region and to permit an accurate comparison of the isostatic anomalies obtained in this investigation with those deducing using the Airy-Heiskanen method. The section is 720 km long, (*see* Figure 1), and the analysis has been completed for fifteen grid points at intervals of 51.5 km.

The data and calculated results are shown in Table IV and Figure 9. The mean elevation along the section is 1,850 m and thus the mean depression of the crust is 8.25 km. Condition (36) gives d=48 km for D=40 km, (*see* Table V). The depth obtained for this rather local region is 5 km greater than the value obtained for the Canadian Shield.

Isostatic anomalies using the Airy-Heiskanen method assuming a crustal thickness, D=40 km, have already been calculated for this region and a study of their geological implications carried out by Garland and Tanner (1957). The anomalies for a number of their stations have been included in Figure 9 for comparison with the present results. Examination shows that the two methods are in excellent agreement. The greatest discrepancy is found for Vancouver and Calgary. Disagreement in the results for these stations is not altogether unexpected since both are end points of the profile and therefore subject to much larger uncertainties, as mentioned in a previous section.

The general negative trend of the isostatic anomaly in this region has already been discussed. However, since the grid interval is rather small the local geological effects cannot be entirely eliminated. For example, the large positive anomaly near Banff appears to be a local feature.

TABLE V

$\Sigma(\Delta g_{iso})^2$ for the Cordilleran Section

d(km)	Zero elevation thickness D(km)	$\Sigma(\Delta g_{iso})^2$
30	21.8	13513
40	31.8	11563
50	41.8	10954
56.5	48.2	11095

SECTION III

THREE-DIMENSIONAL ANALYSIS FOR WESTERN CANADA

Method for Three-Dimensional Analysis

The method for the two-dimensional analysis can easily be extended to the three-dimensional problem. The results are reduced as below to evaluate the following overlapping summations:

Subterranean mass distribution

$$\Delta M(a,b) = \frac{1}{2\pi\gamma} \sum_i \sum_j B_{ij}\, \phi^{(1)}_{a-i,\, b-j}, \tag{38}$$

isostatic gravity compensation

$$\Delta g'(a,b) = -2\pi\gamma\rho \sum_i \sum_j H_{ij}\, \phi^{(2)}_{a-i,b-j}, \tag{39}$$

anomaly in the vertical gradient of gravity

$$\Delta\left(\frac{\partial g}{\partial z}\right) = -\frac{\pi}{L} \sum_i \sum_j B_{ij}\, \phi^{(3)}_{a-i,b-j}\,. \tag{40}$$

The components of the deflection of the vertical x-direction:

$$\xi = -\frac{1}{g} \sum_i \sum_j (\Delta g_{iso})_{ij}\, \phi^{(4)}_{a-i,b-j,x}$$

y-direction:

$$\eta = -\frac{1}{g} \sum_i \sum_j (\Delta g_{iso})_{ij}\, \phi^{(4)}_{a-i,b-j,y}\,. \tag{41}$$

Undulations (relative) of the isostatic geoid

$$\zeta = \frac{1}{g} \sum_i \sum_j (\Delta g_{iso})_{ij}\, \phi^{(5)}_{a-i,b-j} \tag{42}$$

with

$$\phi^{(1)}_{a,b} = \int_0^1 \int_0^1 \cos ma\pi \cos nb\pi\, e^{c\pi\sqrt{m^2+n^2}}\, dm\, dn \tag{43}$$

$$\phi^{(2)}_{a,b} = \int_0^1 \int_0^1 \cos ma\pi \cos nb\pi e^{-c\pi\sqrt{m^2+n^2}}\, dm\, dn \tag{44}$$

$$\phi^{(3)}_{a,b} = \int_0^1 \int_0^1 \sqrt{m^2+n^2}\, \cos ma\pi \cos nb\pi\, dm\, dn \tag{45}$$

$$\phi^{(4)}_{a,b,x} = \int_0^1 \int_0^1 \frac{m}{\sqrt{m^2+n^2}} \sin ma\pi \cos nb\pi\, dm\, dn$$

$$\phi^{(4)}_{a,b,y} = \int_0^1 \int_0^1 \frac{n}{\sqrt{m^2+n^2}} \cos ma\pi \sin nb\pi\, dm\, dn \tag{46}$$

$$\phi^{(5)}_{a,b} = \int_0^1 \int_0^1 \frac{1}{\sqrt{m^2+n^2}} \cos ma\pi \cos nb\pi\, dm\, dn, \tag{47}$$

where a and b are any integer defined by $x = a\pi$, $y = b\pi$. The ratio of the thickness of the crust d to the grid interval L is given by

$$c = \frac{d}{L}$$

along the x and y directions.

By partial integration it can easily be shown that

$$\phi^{(4)}_{a,b,x} = a\pi\, \phi^{(3)}_{a,b}$$

$$\phi^{(4)}_{a,b,y} = -b\pi\, \phi^{(3)}_{a,b}\,.$$

Evaluation of other $\phi^{(k)}_{a,b}$ must be carried out by numerical integration. However, the numerical integration of $\phi^{(5)}_{a,b}$ presents a difficulty because it has a singular point at $m=0$, $n=0$. Thus the undulation of the geoid ζ was calculated by a graphical integration of the components of the deflection of the vertical ξ and η as shown later. Several properties of the integrals $\phi^{(k)}_{a,b}$ may be noted as follows:

Symmetry

$$\phi^{(1,2,3)}_{a,b} = \phi^{(1,2,3)}_{b,a} = \phi^{(1,2,3)}_{-a,b} = \phi^{(1,2,3)}_{a,-b}$$

$$\phi^{(4)}_{b,a,x} = \phi^{(4)}_{a,b,y}\ ;\ \phi^{(4)}_{b,a,y} = \phi^{(4)}_{a,b,x}$$

$$\phi^{(4)}_{a,-b,x} = \phi^{(4)}_{a,b,y}\ ;\ \phi^{(4)}_{a,-b,y} = -\phi^{(4)}_{a,b,y}$$

$$\phi^{(4)}_{-a,b,x} = -\phi^{(4)}_{a,b,x}\ ;\ \phi^{(4)}_{-a,b,y} = \phi^{(4)}_{a,b,y}, \tag{48}$$

convergency

$$\sum_{a=-\infty}^{\infty} \sum_{b=-\infty}^{\infty} \phi^{(1)}_{a,b} =$$

$$\sum_{a=-\infty}^{\infty} \sum_{b=-\infty}^{\infty} \phi^{(2)}_{a,b} = 1$$

$$\sum_{a=-\infty}^{\infty} \sum_{b=-\infty}^{\infty} \phi^{(3)}_{a,b} =$$

$$\sum_{a=-\infty}^{\infty} \sum_{b=-\infty}^{\infty} \phi^{(4)}_{a,b,x} =$$

$$\sum_{a=-\infty}^{\infty} \sum_{b=-\infty}^{\infty} \phi^{(4)}_{a,b,y} = 0. \tag{49}$$

Evaluation of $\phi^{(1)}_{a,b}$, $\phi^{(2)}_{a,b}$, $\phi^{(3)}_{a,b}$, and $\phi^{(4)}_{a,b,x,y}$ for $c = \frac{1}{2}$ and a, b ranging from $0 \sim \pm 15$ have been carried out using the Gaussian method of numerical integration. Details concerning this phase of the project in which a digital computer (Datatron 205) was employed are

given in Appendix A. The results of the integration $\phi^{(1)}{}_{a,b}$, $\phi^{(2)}{}_{a,b}$, $\phi^{(3)}{}_{a,b}$, $\phi^{(4)}{}_{a,b,x}$ are tabulated in Appendices B, C, D, and E. With the aid of the numerical tables $\phi^{(k)}{}_{a,b}$ it is possible to apply a three-dimensional analysis to any area in which gravity and elevation data are available. Of course the tables are only for the special case

$$c = \frac{d}{L} = \tfrac{1}{2}.$$

Thus it is necessary to assume or infer by other means the thickness of the crust and then determine the grid interval to be used in the analysis.

The convergence of $\phi^{(k)}{}_{a,b}$ is satisfactory for the present problem as can be seen from Table VI.

TABLE VI

Convergencies of the Integrals $\phi^{(k)}_{a,b}$

	$\phi^{(1)}_{a,b}$	$\phi^{(2)}_{a,b}$	$\phi^{(3)}_{a,b}$
$\sum_{-1}^{+1}\sum_{-1}^{+1}$	0.77846	0.74499	0.11100
$\sum_{-3}^{+3}\sum_{-3}^{+3}$	1.01090	0.87843	0.07554
$\sum_{-5}^{+5}\sum_{-5}^{+5}$	1.04298	0.92078	0.04543
$\sum_{-10}^{+10}\sum_{-10}^{+10}$	1.03254	0.95659	0.02923
$\sum_{-15}^{+15}\sum_{-15}^{+15}$	1.02425	0.97094	0.01814

An evaluation of $\phi^{(1)}{}_{a,b}$ for values of a and b between ± 15, for $c=1$ and $c=\frac{1}{2}$ has been carried out by Tsuboi, Oldham and Waithman (1958) using Weddle's method of numerical integration. The values for $\phi^{(1)}{}_{a,b}$ obtained in this paper agree with those by these investigators within the fourth decimal place.

To complete the synthesis the overlapping summations defined by (38) to (41) must be carried out. The required matrix products expressed in practical units are listed below. The following constants have been used:

gravitational constant: $= 6.670 \times 10^{-8}$ dynes/cm²/gm²

density of the crust: $= 2.67$ gm/cm³

density of the subterranean mantle: $= 3.27$ gm/cm³

depth of the crust: $d = 36$ km

grid interval: $L = 72$ km.

Subterranean mass distribution

$$\Delta M(a,b) = 2.386 \times 10^{3} \sum_i \sum_j B_{ij}\, \phi^{(1)}{}_{a-i,b-j} \text{ gm/cm}^2$$

(B_{ij} in units of mgals).

Boundary relief

$$h(a,b) = 39.76 \times 10^{-2} \sum_i \sum_j B_{ij}\, \phi^{(1)}{}_{a-i,b-j} \text{ km.}$$

A positive value indicates an abnormally thick crust.

Isostatic mass anomaly

$$\Delta M(a,b)_{iso} = \Delta M(a,b) - 2.67\, H \times 10^{3} \text{ gm/cm}^2.$$

Isostatic gravity anomaly

$$\Delta g(a,b)_{iso} = B(a,b) + 1.119 \sum_i \sum_j H_{ij}\, \phi^{(2)}{}_{a-i,b-j} \text{ mgals}$$

(H_{ij} in units of 10 m).

Anomaly in the vertical gradient of gravity

$$\Delta\left(\frac{\partial g}{\partial z}\right) = -4.363 \times 10^{-5} \sum_i \sum_j B_{ij}\, \phi^{(3)}{}_{a-i,b-j} \text{ mgal/m}$$

This value indicates a deviation from the normal value of -3086×10^{-4} mgal/m.

Deflection of the vertical referred to the isostatic geoid

$$\begin{matrix}\text{x-direction: } \xi \\ \text{y-direction: } \eta\end{matrix} = -.2062 \sum_i \sum_j (\Delta g_{iso})_{ij} \begin{matrix}\phi^{(4)}{}_{a-i,b-j,x} \\ \phi^{(4)}{}_{a-i,b-j,y}\end{matrix} \text{ sec.}$$

A digital computer has been used also for carrying out the overlapping summations. Since $\phi^{(k)}{}_{a,b}$ converges to zero as a and b approach infinite values, B_{ij} and H_{ij} at infinity must be known to obtain the exact and absolute values of the matrix products. However gravity and elevation data in the present study are confined to a finite area and for external regions gravity and elevation values are assumed to be zero. It might therefore be expected that the results for grid points near the boundary will have errors. From Table VI it can be seen that even the summation for

$$\sum_{a=-1}^{+1} \sum_{b=-1}^{+1} \phi^{(k)}{}_{a,b}$$

is not far from the convergent limiting value

$$\sum_{-\infty}^{\infty} \sum_{-\infty}^{\infty} \phi^{(k)}{}_{a,b}\,.$$

We may safely conclude, therefore, that for all interior points including those within one grid interval from the boundary, reliable results have been obtained. Only for those points lying on the edge do the results have large uncertainties.

The undulation of the geoid ζ was obtained by integration of ξ and η as follows: In Figure 10 let the components

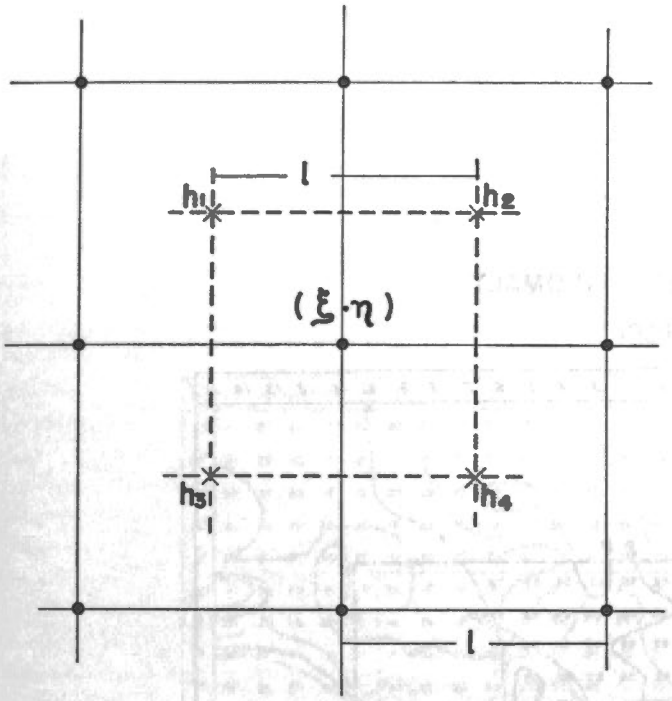

Figure 10. Relation between the deflections of the vertical (ξ , η) and the geoidal heights h at the nearest neighboring grid points in the sub-lattice.

ξ and η of the deflection be known for each grid point. Then approximately,

$$\xi = \frac{1}{2L}(h_2 - h_1 + h_4 - h_3)$$

$$\eta = \frac{1}{2L}(h_1 - h_3 + h_2 - h_4) \qquad (50)$$

where h_1, h_2, h_3, h_4 are the values of geoidal heights for the grid points in the sub-lattice with the grid interval L. Thus we obtain

$$h_2 - h_3 = L(\xi + \eta)$$

or (51)

$$h_4 - h_1 = L(\xi - \eta).$$

Relative to some arbitrarily selected grid point, the variations in geoidal heights can be determined step by step.

Data and Results

In the three-dimensional analysis a crustal thickness of d = 36 km was assumed. This is the thickness obtained in the two-dimensional analysis for the Canadian Shield which overlaps the present area. For $c = \frac{1}{2}$ the grid interval becomes 72 km. The Bouguer gravity anomalies for a rectangular of approximately 900 × 900 miles bounded by latitudes 49 and 62°N and longitudes 90 and 113°W are represented by a grid of 21 × 21 points. This grid system implies that a and b range from 0 to ±10. The central point (a = 0, b = 0) lies close to Flin Flon, Manitoba, (about 55°N, 102°W). The lines b, equal to a constant, are parallel to lines of equal latitude and a, equal to a constant, orthogonal to these. Positive values of a and b indicate the eastern and northern sides respectively. It is pointed out that this rectangular area assumed to be a plane does not correspond to an exact orthogonal network on the actual surface of the earth but is distorted due to curvature. However the effect of this distortion can be neglected in this study.

To improve the values of the isostatic anomalies at points close to the edges elevation data H(a,b) is supplied for a grid of 31 × 31 points thereby extending a and b from ±10 to ±15. Subsequently when gravity data B(a,b) becomes available for the grid points in the extended area the isostatic anomalies can be readily obtained. Figures 11 and 12 give the data for B(a,b) and H(a,b) respectively in a matrix form. For the ocean region of Hudson Bay to the northeast, the H(a,b) data are obtained from the relation: $H\rho_0 = (H - H')\rho$ which effectively replaces seawater of depth H and density ρ_0 by an equivalent layer of rock of thicknesses $H - H'$ and density ρ. Assuming values of 1.03 and 2.67 gm/cm³ for ρ_0 and ρ respectively, the equivalent depth H′ of the oceanic sector is therefore:

$$H' = 0.614\ H. \qquad (52)$$

The values of B(a,b) for the corresponding ocean region are not available and are assumed to be zero.

The geological map for the corresponding area based upon the tectonic map of Canada is shown in Figure 13. It embraces two distinct physiographic-geological provinces, The Canadian Shield, characterized by vast exposures of igneous rocks of Precambrian age and the Central Plains underlain by Palaeozoic and younger sediments. The boundary separating these two contrasting areas lies roughly along the diagonal line from the northwest corner to the southeast corner of the map. Contours of depths below sea level of the Precambrian basement beneath the sedimentary cover are shown at intervals of 1,000 feet. The maximum thickness of sediments indicated is about 6,000 feet (2 km), which is only about 6 per cent of the total crustal thickness.

The results of the calculations are summarized and shown in Figures 14, 15, 16, 17, and 18. It will be noted that in some of these, the contour lines along the margins have been omitted since the accuracy of the computed values along the edges is known to be low.

Figure 14 is a relief map of the base of the crust. For interior grid points the undulations vary from −1.4 to 4.7 km which is about 17 per cent of the average crustal thickness. This analysis shows an anticlinal structure of the crust mantle boundary which parallels the Nelson

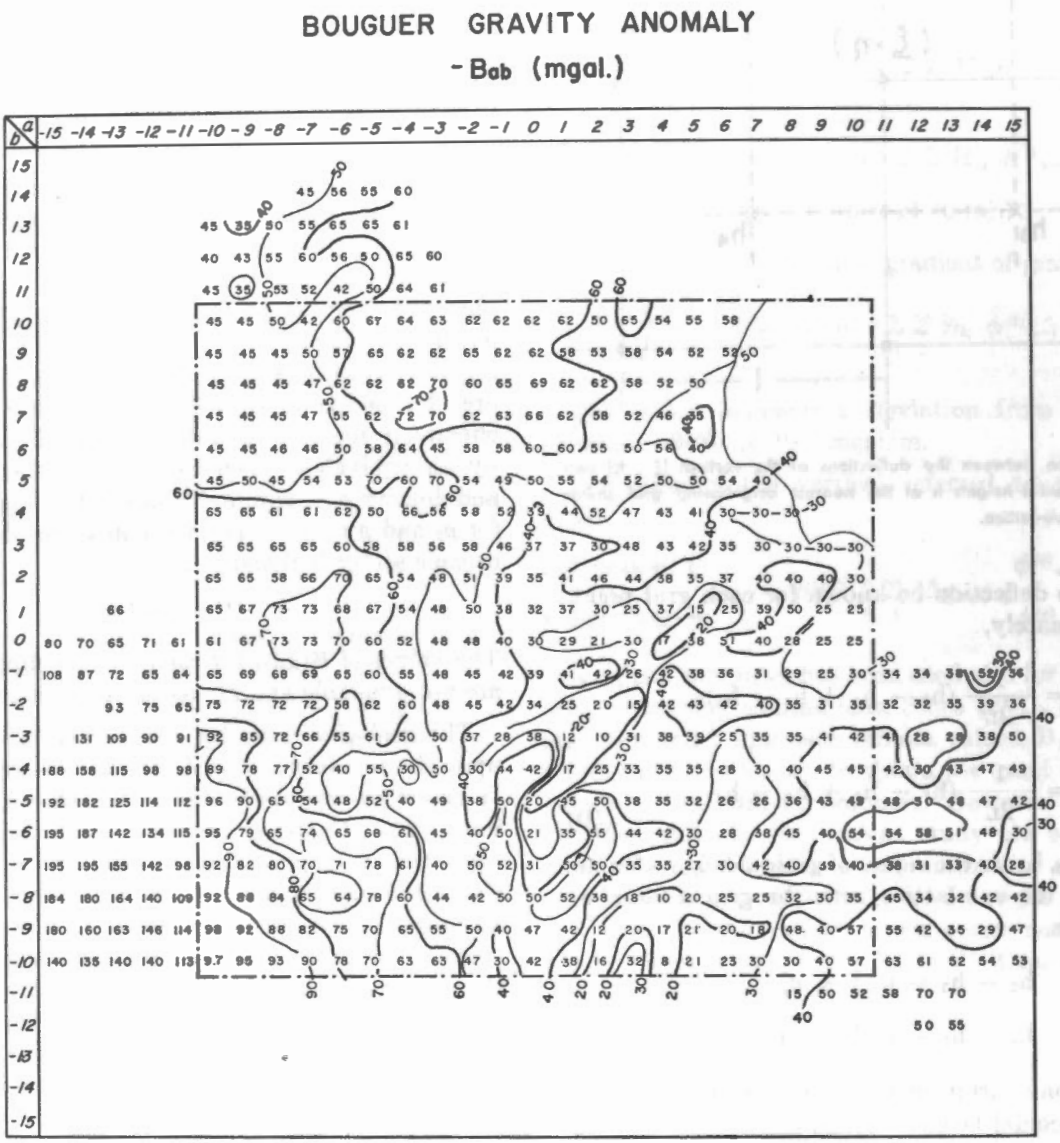

Figure 11. Bouguer gravity anomaly data for the three-dimensional analysis. All the values are negative.

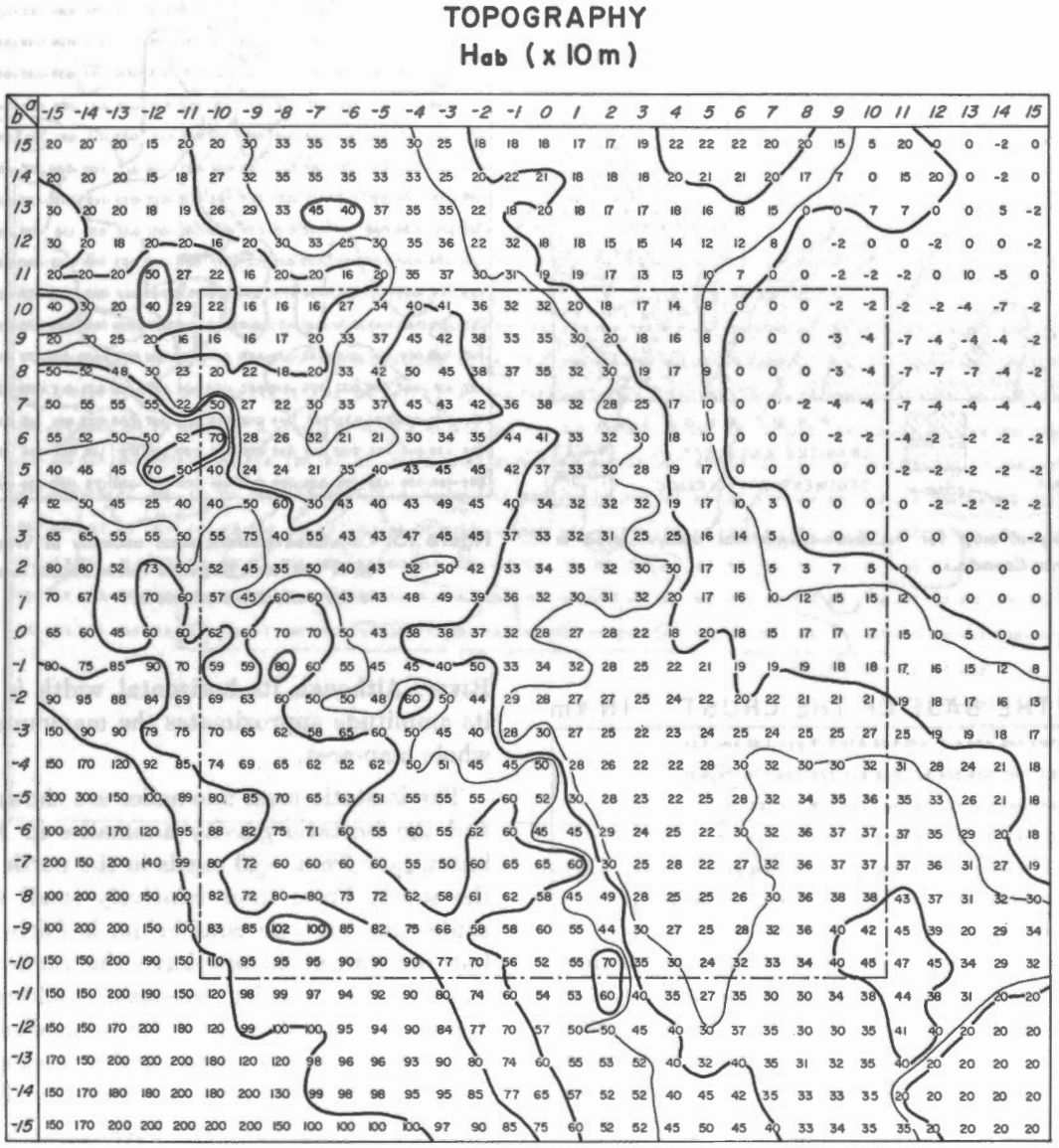

Figure 12. Elevation data for the three-dimensional analysis in units of 10 metres.

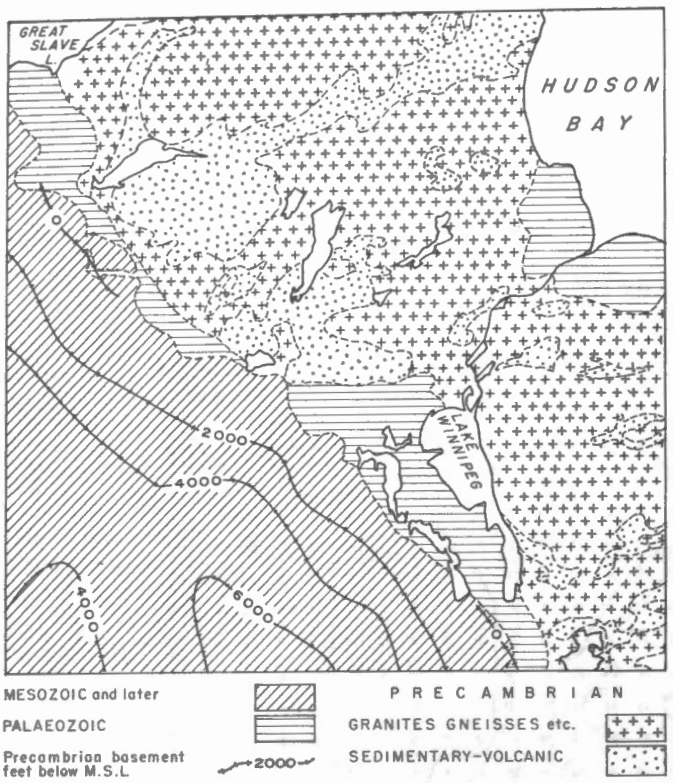

Figure 13. Geological map for the three-dimensional analysis area in Western Canada.

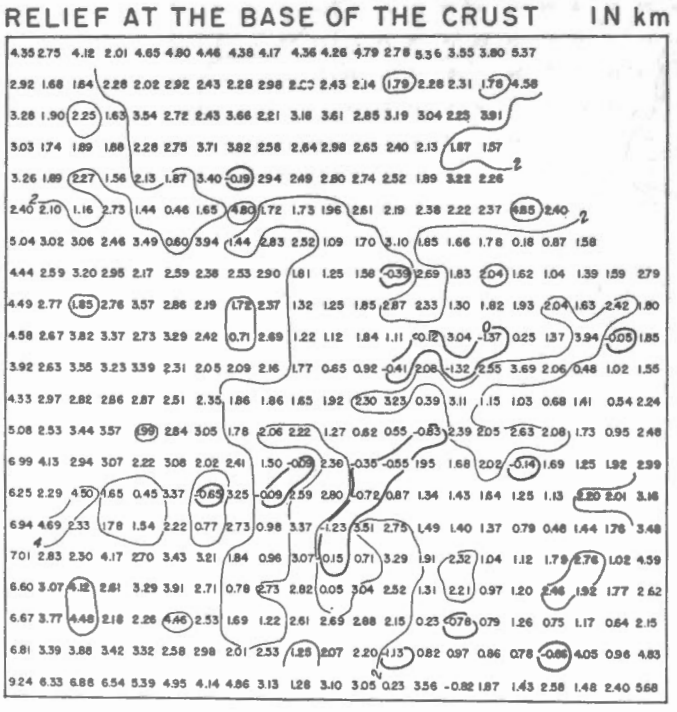

Figure 14. Calculated relief at base of the crust in Western Canada (km), which is the deviation from the normal depth d = 36 km. A positive value means that the crust is thicker than normal.

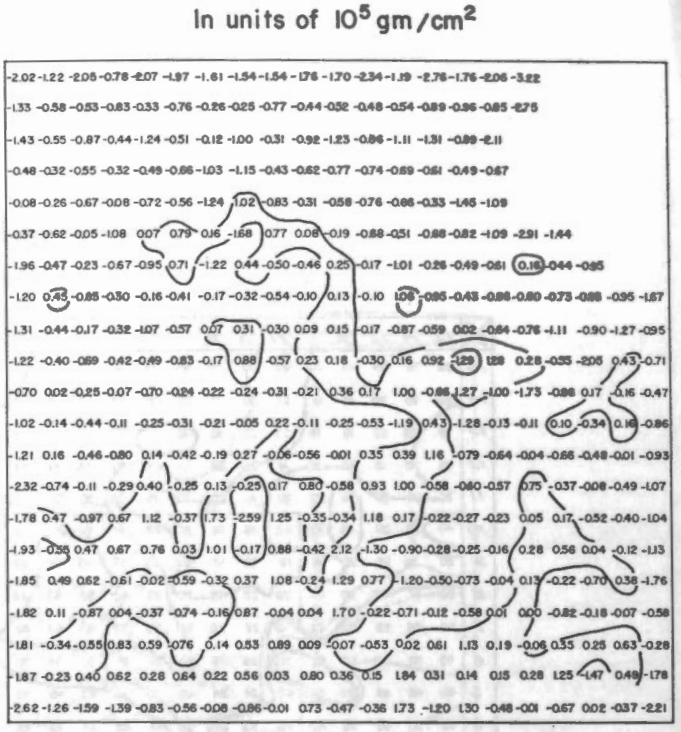

Figure 15. Calculated isostatic mass anomaly in Western Canada (units of 10^5 gm/cm^2). Negative values denote mass defects compared to the perfect isostatic state.

River. Although its horizontal width is only 100 km, its amplitude approximates the maximum value for the whole map-area.

The isostatic mass anomalies are shown in Figure 15, and the isostatic gravity anomalies in Figure 16. The latter vary from −40 mgals in the north to 40 mgals in the south. From these relatively small values we conclude that isostatic equilibrium is fairly well attained, but the values do not have the random distribution expected for complete isostatic equilibrium. The predominantly negative isostatic anomalies to the north indicate over-compensation and a thicker crust for this area; conversely the more positive anomalies to the south suggest under-compensation and a thinner crust. This division corresponds roughly to the two geological provinces, the Precambrian Shield to the north and the Central Plains to the south. The Nelson River feature previously discussed appears more pronounced from the distribution of the isostatic mass anomalies than from the isostatic gravity anomalies. This might be predicted from equations (43) and (44) for these quantities. The former contains a factor

$$\exp\left(c\pi\sqrt{m^2+n^2}\right)$$

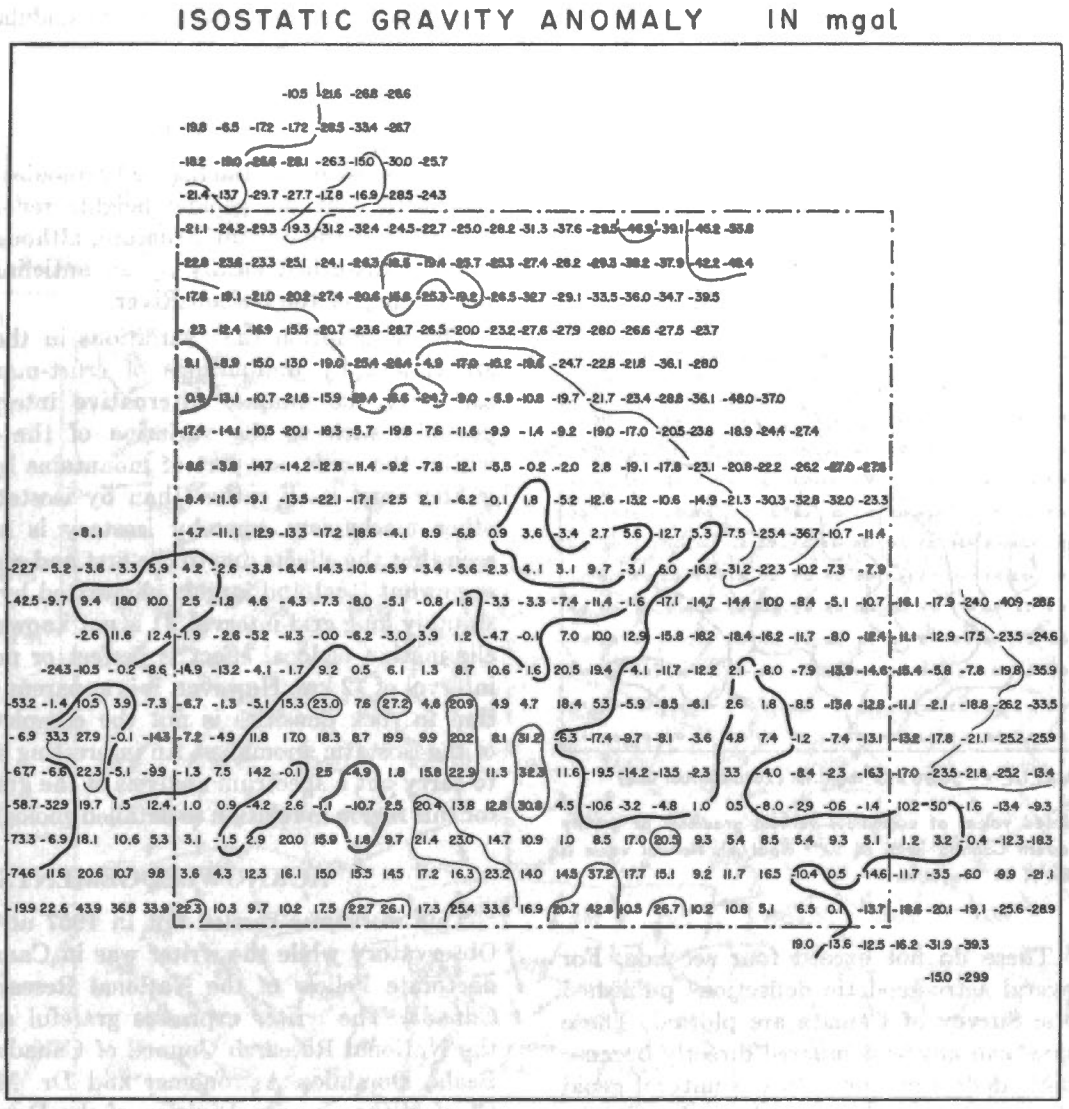

Figure 16. Calculated isostatic gravity in Western Canada (mgals).

which varies more sensitively for the higher harmonics of m and n than for the reciprocal factor

$$\exp\left(-c\pi\sqrt{m^2+n^2}\right)$$

in the expression (44) for the isostatic gravity anomaly. Comparison of gravity calculated from an assumed mass distribution with observed values of gravity seems a suitable method to follow in large scale structural studies; the converse method of calculating the mass distribution or variation in subcrustal relief from the observed gravity anomalies is a more suitable method of analysis to emphasize local structure.

In Figure 17 the vertical gradient of gravity is shown to be numerically smaller or larger than normal within the areas of negative and positive gravity anomalies respectively. However, since the fluctuation is everywhere less than 0.1 per cent, it can be neglected in the free-air reduction of gravity. The fluctuation is small because the local variations of the gravity field are smoothed out, that is, they include no higher harmonics. As seen in expression (45) the vertical gradient contains a term

$$\sqrt{m^2+n^2}$$

and therefore the higher harmonics in the gravity field are much amplified in the distribution of the vertical gradient.

The deflection components ξ and η that have been combined as

$$\sqrt{\xi^2+\eta^2}$$

to give total deflections which are illustrated vectorially

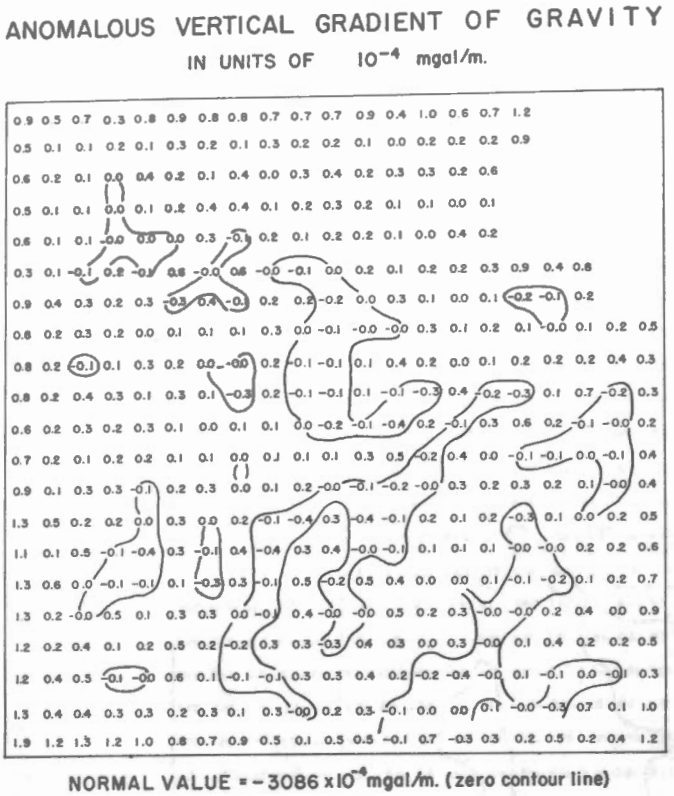

Figure 17. Calculated values of anomalous vertical gradients of gravity in Western Canada (units of 10^{-4} mgal/m). Normal value is -3084×10^{-4} mgal/m.

in Figure 18. These do not exceed four seconds. For comparison several astro-geodetic deflections published by the Geodetic Survey of Canada are plotted. These two sets of values can not be compared directly because the astro-geodetic deflections refer to the natural geoid whereas the computed deflections are derived from isostatic anomalies. It is obvious that the computed deflections show a systematic distribution corresponding to the undulation of geoidal heights. These calculated undulations which are referred to the central grid point in the sub-lattice (*see* Figure 10) have a surprisingly clear dip towards the north, ranging from a maximum of 5 m in the south to a minimum of -7.9 m to the northeast. Since expression (47) for the undulation of geoidal heights has a term

$$\frac{1}{\sqrt{m^2 + n^2}}$$

it is less sensitive to the higher harmonics and it may be concluded that the geoidal heights reflect the general character of the crustal structure, although this general trend is disturbed locally by an anticlinal structure in the vicinity of the Nelson River.

The assumption that variations in the gravity field are caused by undulations of crust-mantle boundary can never be unique. Alternative interpretations are possible, such as the variation of the rock densities within the crust, support of mountains by the strength of the crust itself rather than by isostatic balance, or other mechanism whereby isostasy is achieved. It is seen that the effects due to the first and second should be somewhat local and largely eliminated by adoption of a suitably long grid interval. It is not known whether such elimination of local effect is perfect or not for the grid interval of 72 km. However, it is apparent that the variation in rock densities is not the complete explanation of the isostatic anomalies. An interesting study might be to carry out a spectrum analysis of the gravity variation for this region in relation to detailed geological structures.

ACKNOWLEDGEMENTS

This work was carried out in 1957 at the Dominion Observatory while the writer was in Canada as a Postdoctorate Fellow of the National Research Council of Canada. The writer expresses grateful appreciation to the National Research Council of Canada, to Dr. C. S. Beals, Dominion Astronomer and Dr. M. J. S. Innes, Chief of the Gravity Division of the Dominion Observatory, and to the staff of Burroughs Business Machines Ltd. Thanks are tendered also to Drs. C. H. G. Oldham and V. B. Waithman for the use of their unpublished numerical tables for $\phi^{(1)}_{a,b}$.

The writer is especially indebted to Dr. Innes for his help and criticism throughout the course of the investigation and preparation of the manuscript.

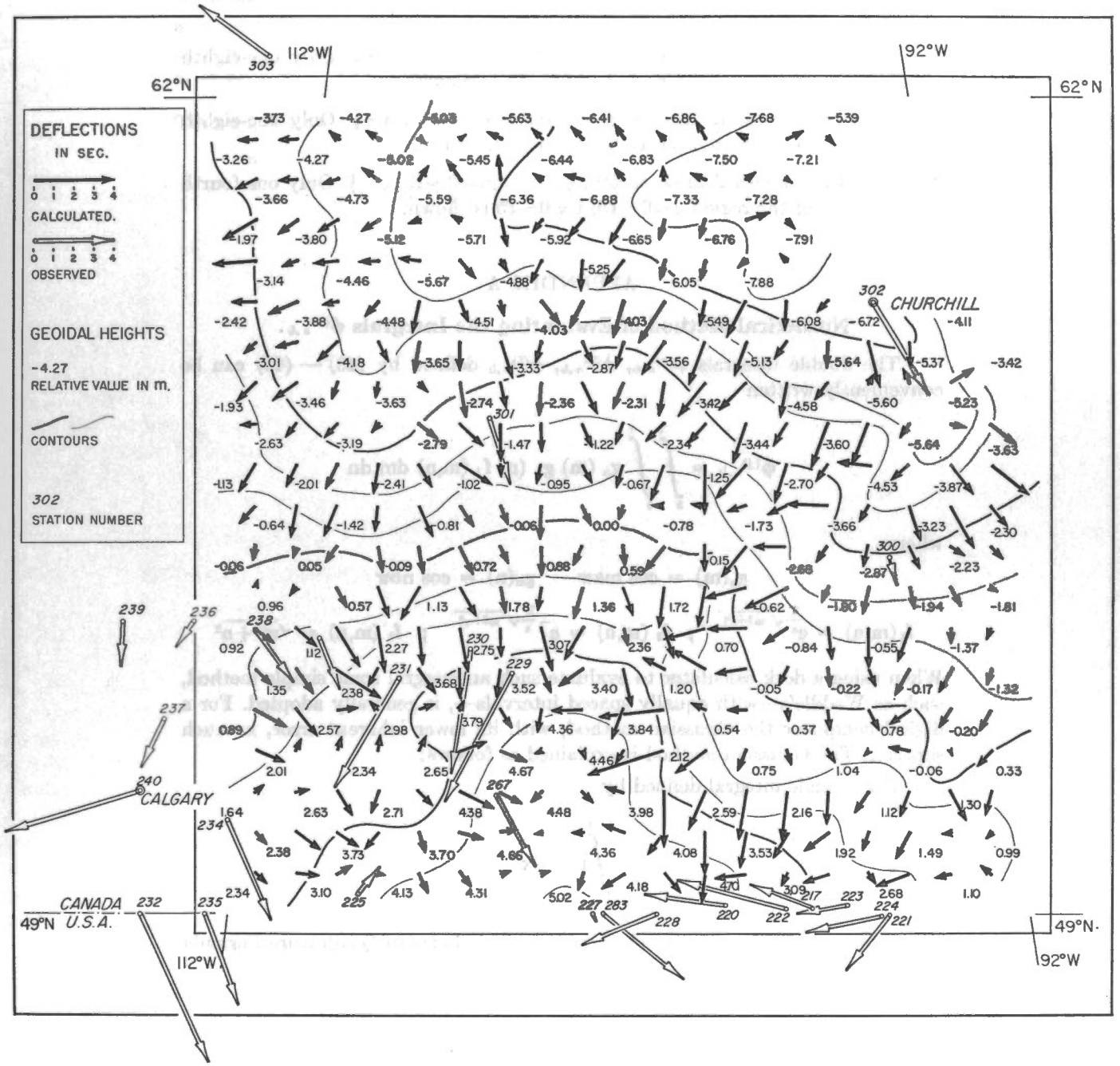

Figure 18. Calculated deflections of the vertical referred to the isostatic geoid, and undulations in geoidal heights relative to a central grid-point near Flin Flon, Manitoba. Deflections (uncorrected for isostatic compensation) observed by the Geodetic Survey of Canada are also shown vectorially; the inwardly directed normal is indicated.

APPENDICES

Appendix A. Numerical method of evaluating the integrals $\phi^{(k)}{}_{a,b}$.

Appendix B. Numerical table of $\phi^{(1)}{}_{a,b}$ for a,b=0∼15 and c=½. Due to the symmetrical property, it is sufficient to show only one-eighth of the region for a=0∼15; b≤a.

Appendix C. Numerical table of $\phi^{(2)}{}_{a,b}$ for a,b=0∼15, c=½. Only one-eighth of the region for a=0∼15; b≤a is shown.

Appendix D. Numerical table of $\phi^{(3)}{}_{a,b}$ for a,b=0∼15, c=½. Only one-eighth of the region for a=0∼15, b≤a is shown.

Appendix E. Numerical table of $\phi^{(4)}{}_{a,b,x}$ for a,b=0∼15, c=½. Only one-fourth of the region a=0∼15, b=0∼15 is shown.

APPENDIX A

Numerical Method of Evaluating the Integrals $\phi^{(k)}{}_{a,b}$.

The double integrals $\phi^{(1)}{}_{a,b}$, $\phi^{(2)}{}_{a,b}$, $\phi^{(3)}{}_{a,b}$ defined by (43) — (45) can be conveniently written

$$\phi^{(j)}{}_{a,b} = \int_0^1 \int_0^1 g_a(m)\, g_b(n)\, f_j(m,n)\, dm\, dn$$

where

$$g_a(m) = \cos ma\pi \qquad g_b(n) = \cos nb\pi$$

$$f_1(m,n) = e^{\pi\sqrt{m^2+n^2}} \;;\; f_2(m,n) = e^{-\pi\sqrt{m^2+n^2}} \;;\; f_3(m,n) = \sqrt{m^2+n^2}$$

When using a desk calculator to evaluate such an integral some simple method, such as Weddle's—with equally spaced intervals—, is generally adopted. For a digital computor the Gaussian method, with its lower inherent error, is much superior. The Gaussian method is explained as follows:

For a single integral defined by

$$\int_{-1}^{1} f(x)\, dx$$

the abscissae a_i and weight coefficient H_i for the Gaussian Quadrature Formula are tabulated for the following form

$$\int_{-1}^{1} f(x)dx = \sum_{i=1}^{n} H_i\, f(a_i).$$

To make the necessary transformation let

$$m_i,\, n_i = \frac{a_i + 1}{4} \qquad i = 0 \sim 9 \qquad \frac{a_i + 3}{4} \qquad i = 10 \sim 19\,.$$

A twenty-abscissae point Gaussian method is used. Unfortunately the weight coefficients for twenty points have not been tabulated and so the ten-point formula

has been applied to each of the intervals $(0,\frac{1}{2})$ and $(\frac{1}{2},1)$. The abscissae a_i and weight function H_i for ten points are given as follows:

	a_i		H_i
$a_1 = a_{10}$	0.97390 65285 17172	$H_1 = H_{10}$	0.06667 13443 08688
$a_2 = a_9$	0.86506 33666 88985	$H_2 = H_9$	0.14945 13491 50581
$a_3 = a_8$	0.67940 95682 99024	$H_3 = H_8$	0.21908 63625 15982
$a_4 = a_7$	0.43339 53941 29247	$H_4 = H_7$	0.26926 02109 27734
$a_5 = a_6$	0.14887 43389 81631	$H_5 = H_6$	0.29552 42247 14753

Then applying the above formula twice we get the formula to evaluate $\phi^{(j)}{}_{a,b}$ as

$$\phi^{(j)}{}_{a,b} = \sum_{l=0}^{19} H_l \cdot g_b(n_l) \sum_{k=0}^{19} g_a(m_k) \cdot f_j(m_k, n_l) \quad .$$

APPENDIX B
Numerical Table of $\phi^{(1)}_{a,b} \times 10^6$

b \ a	0	1	2	3	4	5	6	7	8	9	10	11	12	13	14	15
0	3656821	741483−	191531	94780−	51090	34306−	23128	17506−	13078	10552−	8381	7076−	5862	5037−	4228	3328−
1		21895	19403−	3408	4486−	1570	1827−	855	996−	566	610−	369	408−	288	315−	210
2			442	3449−	135	1159−	166	570−	113	274−	79	199−	81	134−	48	91−
3				202−	1121−	34−	494−	33−	235−	0	148−	5−	86−	20	77−	17
4					99−	502−	93−	233−	45−	126−	44−	72−	8−	61−	1−	40−
5						130−	253−	66−	111−	74−	58−	25−	51−	23−	40−	7−
6							80−	100−	90−	66−	48−	31−	42−	37−	0	30−
7								90−	63−	73−	22−	50−	39−	12−	18−	12−
8									75−	13−	52−	29−	26−	24−	12−	35−
9										52−	27−	34−	19−	10−	43−	2−
10											46−	25−	2−	39−	1	20−
11												6−	37−	1	39−	18
12													4	45−	16	42−
13														26	39−	13
14															25	39−
15																12

APPENDIX C
Numerical Table of $\phi^{(2)}_{a,b} \times 10^6$

b \ a	0	1	2	3	4	5	6	7	8	9	10	11	12	13	14	15
0	333456	74523	3225	5457	269−	1584	306−	721	216−	403	159−	260	122−	176	95−	74
1		28338	5575	2923	831	776	217	322	79	163	31	100	11	63	4	25
2			3442	1612	900	486	320	201	147	93	79	55	45	32	31	21
3				1049	613	401	256	186	123	94	69	57	39	34	27	23
4					437	296	216	148	111	82	66	48	39	31	27	21
5						231	166	124	92	76	55	44	36	31	24	21
6							130	97	82	63	50	39	35	27	21	19
7								83	67	55	42	37	31	24	19	18
8									56	43	38	32	27	22	20	17
9										38	33	28	22	20	17	15
10											30	24	20	19	16	12
11												20	19	17	15	11
12													17	15	12	12
13														11	11	11
14															9	10
15																9

APPENDIX D
Numerical Table of $\phi^{(n)}_{a,b} \times 10^6$

b \ a	0	1	2	3	4	5	6	7	8	9	10	11	12	13	14	15
0	765186	138403–	16213	11840–	4804	3983–	2249	1973–	1302	1173–	843	777–	593	549–	432	313–
1		25144–	2994–	2315–	318–	643–	44–	277–	5	149–	16	92–	16	61–	17	27–
2			2447–	985–	619–	291–	223–	114–	103–	55–	56–	30–	34–	17–	21–	11–
3				709–	380–	272–	157–	123–	75–	64–	41–	38–	24–	24–	15–	16–
4					294–	184–	141–	92–	74–	50–	43–	30–	27–	19–	18–	13–
5						149–	102–	83–	58–	48–	35–	30–	22–	20–	15–	13–
6							86–	63–	52–	39–	33–	25–	22–	17–	15–	12–
7								54–	41–	35–	27–	24–	18–	16–	13–	11–
8									36–	28–	25–	20–	17–	14–	12–	10–
9										25–	20–	18–	15–	13–	11–	10–
10											18–	15–	14–	11–	10–	9–
11												14–	12–	11–	9–	8–
12													11–	9–	8–	7–
13														8–	7–	7–
14															7–	6–
15																5–

APPENDIX E
Numerical Table of $\phi^{(4)}_{a,b,z} \times 10^6$

b \ a	0	1	2	3	4	5	6	7	8	9	10	11	12	13	14	15
0	0	0	0	0	0	0	0	0	0	0	0	0	0	0	0	0
1	434806	78992	9404	7272	999	2019	138	870	15−	469	49−	289	51−	192	53−	84
2	101872−	18810	15374	6191	3891	1828	1404	719	649	342	352	185	212	108	135	68
3	111589	21817	9286	6685	3579	2563	1475	1160	706	607	382	354	226	224	144	148
4	60371−	3998	7782	4772	3697	2311	1778	1157	935	632	539	374	335	237	222	165
5	62568	10094	4570	4272	2889	2343	1608	1298	913	758	547	471	348	309	232	211
6	42389−	828	4213	2950	2667	1929	1617	1811	986	732	622	471	410	315	281	221
7	43377	6089	2516	2707	2025	1817	1377	1183	903	773	597	517	405	357	283	251
8	32715−	118−	2595	1884	1869	1461	1314	1032	903	713	622	496	436	351	312	255
9	33175	4220	1541	1822	1422	1365	1098	994	802	712	577	511	417	372	306	273
10	26474−	488−	1762	1272	1347	1095	1037	853	777	641	576	477	427	356	320	270
11	26834	3173	1018	1299	1029	1036	863	813	682	625	525	476	401	367	307	278
12	22342−	609−	1274	905	1005	834	819	695	653	556	513	437	400	342	312	269
13	22424	2495	704	971	770	804	683	662	570	537	462	429	370	341	295	270
14	19014−	742−	944	670	778	650	655	567	545	475	448	391	364	318	294	259
15	14751	1260	511	742	619	632	554	538	479	455	405	379	337	312	278	256

Bibliography

GARLAND, G. D. AND TANNER, J. G.
1957: Investigations of gravity and isostasy in the southern Canadian Cordillera. *Dom. Obs. Pub.*, Ottawa, v. 19, no. 5.

HAYFORD, J.
1909: The figure of the earth and isostasy from measurements in the United States. U.S. Coast and Geodetic Survey.

HEISKANEN, W. A.
1957: General report on the gravimetric computation of the undulations of the geoid. N_E. and the deflection of the vertical components ξ_E and η_E. Presented at the 11th General Assembly of the IUGG, Toronto, September 1957.

HODGSON, J. H.
1953: A seismic survey in the Canadian Shield. *Dom. Obs. Pub.*, Ottawa, v. 16, no. 5, 169.

INNES, M. J. S.
1960: Gravity and isostasy in northern Ontario and Manitoba. *Dom. Obs. Pub.*, Ottawa, v. 21, no. 6.

INNES, M. J. S. AND THOMPSON, L. G. F.
1953: The establishment of primary gravimeter bases in Canada. *Dom. Obs. Pub.*, Ottawa, v. 16, no. 8, 281.

MILLER, A. H. AND HUGHSON, W. G.
1936: Gravity and isostasy in Canada. *Dom. Obs. Pub.*, Ottawa, v. 11, no. 3, 81.

NEY, C. H.
1952: Contours of the geoid for southern Canada. *Bull. Géod.* v. 23, 73.

PIZETTI, P.
1911: Sopro il calcolo teorico delle deviazioni del Geoide dall'Ellissoide. *Atti. Acad. Sci. Torino*, v. 46, 331.

RICE, D. A.
1952: Deflections of the vertical from gravity anomalies. *Bull. Géod.* v. 23, 285.

ROSS, J. E. R.
1957: Geodetic operations in Canada, Jan. 1, 1954 to Dec. 31, 1956. Report presented at 11th General Conf. IUGG, Toronto.

STOKES, C. G.
1849: On the variation of gravity and the surface of the earth. *Cambridge Phil. Trans.*, v. 8, 672.

THOMPSON, L. G. D. AND GARLAND, G. D.
1957: Gravity measurements in Quebec, south of latitude 52°N. *Dom. Obs. Pub.*, Ottawa, v. 19, no. 4.

TOMODA, Y. AND AKI, K.
1955: Use of the function $\frac{\sin x}{x}$ in gravity problems. *Japan Acad. Proc.*, v. 31, no. 7, 443.

TSUBOI, C.
1937: The deflections of the vertical, the undulation of the geoid, and gravity anomalies. *Earthquake Res. Inst. Bull.* v. 15, 650, Tokyo.
1938a. Gravity anomalies and the corresponding subterranean mass distributions. *Imp. Acad. Proc.*, Tokyo, v. 14, 170.
1938b. A simple method of approximately determining the thickness of the isostatic earth's crust. *Earthquake Res. Inst. Bull.* v. 16, 285, Tokyo.
1938c. On the hypothesis of Airy and Pratt on isostasy. *Zisin, J. Seismol Soc.* Japan, ser. 1, v. 10, 109.
1939. Relation between gravity values and corresponding subterranean mass distributions, III. *Earthquakes Res. Inst. Bull.* v. 17, 351, Tokyo.
1940: Relation, etc., V. Isostatic anomalies and the isostatic geoid in USA. *Earthquake Res. Inst. Bull.* v. 18, 384, Tokyo.
1942: Relation, etc. VII, (in Japanese) *Earthquake Res. Inst. Bull.* v. 20, 30, Tokyo.
1942: Relation, etc. VIII, (in Japanese) *Earthquake Res. Inst. Bull.* v. 20, 149, Tokyo.
1948: Undulation of the isostatic geoid in the East Indies as calculated from gravity anomalies. *Geophys. Notes*, Tokyo Univ., *40*.
1949: The direct and indirect methods for determining the thickness of the isostatic earth's crust. *Geophys. Notes*, Tokyo Univ., *2*, No. 4.
1950: Thickness of the isostatic earth's crust in various parts of USA. *Geophys. Notes*, Tokyo Univ., *3*, No. 5.
1954a: A new and simple method for calculating the deflection of the vertical from gravity anomalies. *Japan Acad. Proc.* v. 30, no. 6, 461.
1954b: A study of the anomalies in the vertical gradient of gravity with the aid of the Bessel-Fourier series. *Japan Acad. Proc.*, v. 30, no. 6, 453.

TSUBOI, C. AND FUCHIDA, T.
1937: Relation, etc. I. *Earthquake Res. Inst. Bull.* v. 15, 636, Tokyo.
1938: Relation, etc. II, *Earthquake Res. Inst. Bull.* v. 16, 273, Tokyo.

TSUBOI, C. AND HAYATSU, A.
1954: A simple method for calculating the deflection of the vertical from gravity anomalies with its applications to 16 selected stations in USA. *J Phys. Earth* v. 2, no. 2, 45.

TSUBOI, C., KANEKO, K., MIYAMURA, S., AND YABASI, T.
1939: Relation, etc. IV. *Earthquake Res. Inst. Bull.* v. 17, 385, Tokyo.

TSUBOI, C., OLDHAM, C. H. G., AND WAITHMAN, V. B.
1958: Numerical tables facilitating three-dimensional gravity interpretations. *J. Phys. Earth*, v. 6, no. 1, 7.

TSUBOI, C. AND YAMAGUTI, S.
1941: Relation, etc. VI. *Earthquake Res. Inst. Bull.* v. 19, 26.

VOS VAN STEENWIJK, J. S., BARON DE.
1946: Plumbline deflections and geoid in Eastern Indonesia. *Neth. Geod. Comm., Pub.*, Waltman, Delft.

VENING MEINESZ, F. A.
1928: A formula expressing the deflection of the vertical in the gravity anomalies and some formulas for the gravity field and the gravity potential outside the geoid. *Koninkl Nederland Akad. Wetens.*, v. 31, no. 3.

WOOLLARD, G. P.
1943: Transcontinental gravitational and magnetic profile of North America and its relation to geologic structure. *Geol. Soc. Am. Bull.* v. 54, 747.